

# Dalton Transactions

An international journal of inorganic chemistry

Accepted Manuscript

This article can be cited before page numbers have been issued, to do this please use: D. Morales-Morales, H. Valdes, J. M. German-Acacio and G. van Koten, *Dalton Trans.*, 2022, DOI: 10.1039/D1DT03870B.



This is an Accepted Manuscript, which has been through the Royal Society of Chemistry peer review process and has been accepted for publication.

Accepted Manuscripts are published online shortly after acceptance, before technical editing, formatting and proof reading. Using this free service, authors can make their results available to the community, in citable form, before we publish the edited article. We will replace this Accepted Manuscript with the edited and formatted Advance Article as soon as it is available.

You can find more information about Accepted Manuscripts in the [Information for Authors](#).

Please note that technical editing may introduce minor changes to the text and/or graphics, which may alter content. The journal's standard [Terms & Conditions](#) and the [Ethical guidelines](#) still apply. In no event shall the Royal Society of Chemistry be held responsible for any errors or omissions in this Accepted Manuscript or any consequences arising from the use of any information it contains.

# Bimetallic Complexes that merge Metallocene and Pincer-Metal Building Blocks: Synthesis, Stereochemistry and Catalytic Reactivity

View Article Online  
DOI: 10.1039/D1DT03870BHugo Valdés,<sup>\*,a</sup> Juan M. Germán-Acacio,<sup>\*,b</sup> Gerard van Koten,<sup>\*,c</sup> and David Morales-Morales<sup>\*,d</sup><sup>a</sup>*Institut de Química Computacional i Catàlisi (IQCC) and Departament de Química, Universitat de Girona, Campus de Montilivi, Girona E-17003, Catalonia, Spain.*<sup>b</sup>*Red de Apoyo a la Investigación, Coordinación de la Investigación Científica-UNAM, Instituto Nacional de Ciencias Médicas y Nutrición SZ, C. P. 14000, Ciudad de México, México.*<sup>c</sup>*Organic Chemistry and Catalysis, Debye Institute for Nanomaterials Science, Faculty of Science, Utrecht University, 3584CG Utrecht, The Netherlands.*<sup>d</sup>*Instituto de Química, Universidad Nacional Autónoma de México, Circuito Exterior, Ciudad Universitaria, Ciudad de México. C. P. 04510, México.*

GvK ORCID 0000-0003-3293-8370; DMM ORCID 0000-0002-7984-1819

## Abstract

This perspective is to illustrate the synthesis and applications of bimetallic complexes by merging a metallocene and a (cyclopentadienyl/aryl) pincer metal complex. Four possible ways to merge metallocene and pincer-metal motifs are reported, see Scheme 1, and representative examples are discussed in more detail. These bimetallic complexes have been employed in some important catalytic reactions such as cross-coupling, transfer hydrogenation or synthesis of ammonia. The metallocene fragment may tune the electronic properties of the pincer ligand, due to its redox reversible properties. Also, the presence of two metals in a single complex allows their electronic communication, which proved beneficial for, e.g., the catalytic activity of some species. The presence of the metallocene fragment provides an excellent opportunity to develop chiral catalysts, because the metallocene merger generally renders the two faces of the pincer-metal catalytic site diastereotopic. Besides, an extra chiral functionality may be added to the bimetallic species by using pincer motifs that are planar chiral, e.g. by using the different substituents of pincer ligand “arms” or non-symmetrical arene groupings. Post-functionalization of pre-formed pincer-metal complexes, *via*  $\eta^6$ -coordination with an areneophile such as  $[\text{CpRu}]^+$  and  $[\text{Cp}^*\text{Ru}]^+$  presents a striking strategy to obtain diastereomeric metallocene-pincer type derivatives, that actually involve half-sandwich metallocenes. This approach offers the possibility to create diastereomerically pure derivatives by using the chiral TRISPHAT anion. The authors hope that this report of the synthetic, physico-chemical properties and remarkable catalytic activities of metallocene-based pincer-metal complexes will inspire other researchers to continue exploring this realm.

**Keywords:** metallocene and half-sandwich complexes, pincer-metal complexes, (chiral) catalysis, bimetallic complexes, ferrocene, ruthenocene, cross-coupling

## 1. Introduction

View Article Online  
DOI: 10.1039/D1DT03870B

Metalloenes belong to a very well-known class of coordination complexes that is defined by the *International Union of Pure and Applied Chemistry* (IUPAC) as; “*organometallic coordination compounds in which one atom of a transition metal such as iron, ruthenium or osmium is bonded to and only to the face of two cyclopentadienyl [ $\eta^5$ -(C<sub>5</sub>H<sub>5</sub>)] ligands which lie in parallel planes. The term should not be used for analogues having rings other than cyclopentadienyl as ligands.*”<sup>1</sup> Ferrocene was the first metallocene to be prepared in the beginning of the 1950’s by Kealy, Pauson and Miller,<sup>2, 3</sup> while its characteristic sandwich structure was elucidated by Fischer and Wilkinson, a few years later.<sup>4, 5</sup>

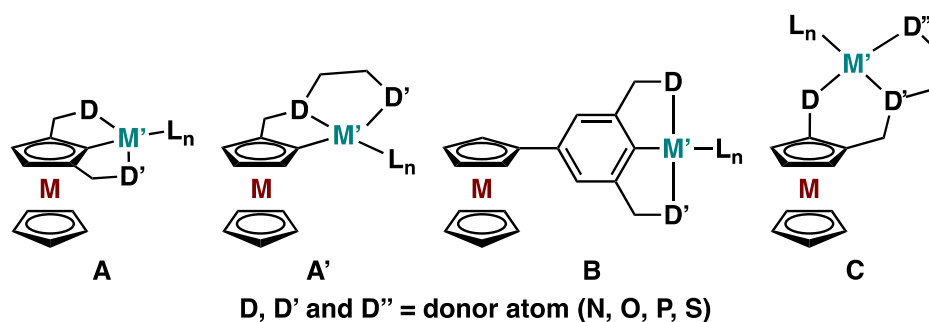
The strong  $\eta^5$ -bonding between the two monoanionic cyclopentadienyl (Cp) ligands and the central metal atom confers to *metalloenes* their high kinetic and thermal stability. For example, most of the metallocenes are robust complexes that are resistant toward moisture and acidic or basic conditions allowing their often easy functionalization.<sup>6, 7</sup> Moreover, metallocenes with, for example, either iron, nickel, osmium, or ruthenium as the central metal atom, exhibit remarkable redox properties. Consequently, metallocenes have been extensively used in a number of fields, ranging from biology, materials science, pharmaceutical applications to chemistry in which the metallocene is used as a building block. In pharmacy, metallocene derived chemicals have been employed as anticancer, antimalarial and radiopharmaceutical agents, as well as, *e.g.*, as biosensors for DNA detection,<sup>8-11</sup> while ferrocene derivatives have been widely used in homogeneous catalysis due to their reversible one-electron redox properties.<sup>12-15</sup> Nevertheless, in terms of produced volume, the most important role of metallocenes is in the realm of catalysis.<sup>16-24</sup> Notably, in polymerization catalysis rather than a genuine metallocene, so-called half-sandwich metallocenes, *i.e.*, metallocenes in which one of the two Cp rings is replaced by other neutral/anionic ligands, have found extensive application.<sup>25-30</sup>

The exploration of complexes with a *pincer-metal platform* is a more recent development although the isolation of the first pincer complexes by Shaw et al already dates back to the mid 1970’s.<sup>31</sup> A pincer-metal complex is defined by the cooperative interaction of the three donor sites of a monoanionic *planar, D, C, D'*-terdentate pincer ligand with the metal center, of which, generally, the binding with the central (mostly carbo-anionic) donor site C is the dominating one. An attractive aspect of a pincer-metal complex is its modular character allowing for the synthesis of a plethora of pincer ligands and, consequently, for fine tuning of the pincer-metal combination. Not surprisingly, like metallocenes, also pincer-metal complexes have found broad application in a great variety of research fields.<sup>32-34</sup> For example, pincer-metal complexes have been used as excellent catalysts for a plethora of transformation in organic synthesis such as hydrogenations, dehydrogenation, cross-coupling, borylations, etc.<sup>35-48</sup>

In view of the orthogonal properties of the metallocene and the pincer-metal platform, combined with the fact that metallocenes are well-accessible to functionalization<sup>6, 7, 30, 49</sup> the question arises; “Could a merger of metallocene and pincer-metal aspects lead to discovery of novel materials with dual properties”? This *Perspectives* explores what already has been

reported and discusses the peculiar effects that have been discovered for these bimetallic species.

View Article Online  
DOI: 10.1039/D1DT03870B



**Scheme 1.** Four possible ways to merge metallocene and pincer-metal motifs: **A**, has the pincer type DCD' manifold integrated along the etch of one of the Cp ligands, **A'**, has only two, D and C, of the three donors integrated, **B**, bears the metallocene unit as a *para*-CpMC<sub>5</sub>H<sub>4</sub> substituent to the arylpincer-M'L<sub>n</sub> unit, and in **C**, a CpMC<sub>5</sub>H<sub>3</sub>-1,2-diyl-grouping is incorporated in the connecting chain of a DD'D''-pincer-M'L<sub>n</sub> unit. Note that other constructs are possible. In section 2*e1* the arylpincer platform is merged with a cationic half sandwich arenophile CpM<sup>+</sup> or Cp\*M<sup>+</sup>.

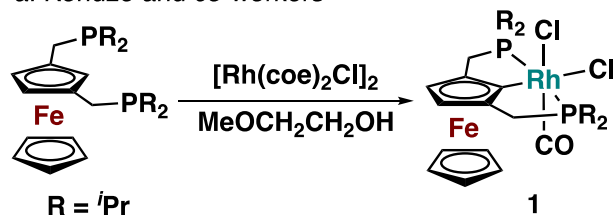
Scheme 1 shows four of the ample routes to merge known motives of a metallocene with that of a pincer-metal complex. In fact, for each of these possibilities examples from the literature are known and will be discussed below. Obvious differences are the short and fixed M···M' distances in **A** and **A'** vs. a much and, yet easy to vary, longer one in **B** (but is fixed because of the rigidity of the connecting spacer) and **C** (having a more flexible arrangement). Firstly, the synthesis and structural features of the various bimetallic complexes **A-C** have been described which is followed by a discussion of the properties and unexpected structural and reactivity features, *e.g.*, resulting from not only electronic interaction between M and M', but also from steric interference and eventually Coulombic effects between the two constituents in these bimetallic metallocene/pincer-metal species.

## 2. Synthetic aspects

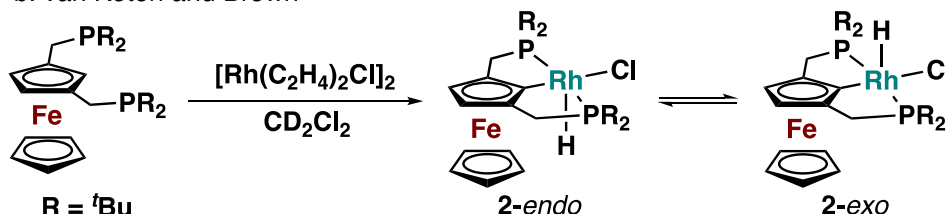
### 2a1. Metallocene-based pincer-metal complexes of type A.

Bimetallic complexes of type **A** were the first ones to be reported. As a metallocene, ferrocene was used that has been substituted, in 1- and 3-position at one of its ferrocenyl rings, with a (dialkylphosphino)methyl substituent. Selective bis*ortho*-cyclometallation with transition metals such as Ir, Rh or Pd *via* direct C-H activation at the Cp ring afforded a ferrocene with an integrated PCP-pincer metal motif, CpFePC<sup>Cp</sup>PM', see Scheme 2.<sup>50-52</sup> Although the mechanism of the C-H activation in metallocene-based pincer complexes is still under-explored it seems likely that the activation of the C-H bond operates through the ionic dissociation/anion-assisted deprotonation route, as was described for the nickelation of PCP- and POCOParyl-pincer ligands.<sup>53</sup>

a. Koridze and co-workers<sup>50</sup>



b. van Koten and Brown<sup>51</sup>



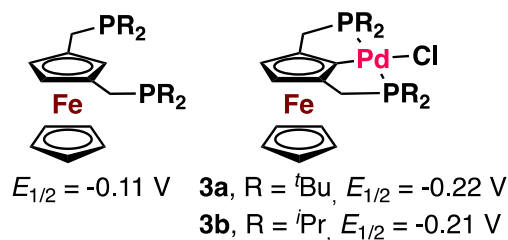
**Scheme 2.** Synthesis of metallocene-based Rh(III)-pincer complexes of the type A.

The solvent used in the reactions may influence the nature of the final metallocene-based pincer complex. For example, Koridze and co-workers reacted 1,3-bis(diphosphinomethyl)ferrocene with  $[\text{Rh}(\text{coe})_2\text{Cl}]_2$  in 2-methoxyethanol at  $120^\circ\text{C}$ , affording a dimetallic complex, **1**, where the rhodium metal fragment exhibits an octahedral geometry, see Scheme 2a.<sup>50</sup> The appearance of CO in the product is likely due to decomposition of the solvent at the applied reaction temperature. To obtain the corresponding  $\text{CpFePC}^{\text{Cp}}\text{PRu}$  derivatives the use of a base such as  $\text{NH}_3$  or  $\text{Et}_3\text{N}$  was required.<sup>54, 55</sup> The choice of the metal precursor is also relevant. For instance, when the preparation of the metallocene-based pincer-complex is carried out with  $[\text{Ru}(\text{PPh}_3)_3\text{Cl}_2]$ , coordination and formation of the ruthenate did not occur, while using  $[\text{Ru}(\text{DMSO})_4\text{Cl}_2]$  the pincer complex was generated in good yields, probably due to the labile character of DMSO as ligand.<sup>54, 55</sup> In contrast, the reaction shown in Scheme 2b was performed in  $\text{CD}_2\text{Cl}_2$  while using  $[\text{Rh}(\text{C}_2\text{H}_4)_2\text{Cl}]_2$  at ambient temperature.<sup>51</sup> The resulting complex **2** is a monohydride species with square pyramidal geometry. In solution, the complex exists as an equilibrium between pair of diastereomers, depending on the position of the hydride ligand. In fact, the steric properties of the P-substituents play also an important role for the formation of the predominant isomer. In the case of  $\text{CpFePC}^{\text{Cp}}\text{PRu}$ -pincer derivatives the presence of tert-butyl groups favored the presence of the *endo*-isomer, while using *iso*-propyl moieties the *exo*-isomer is obtained in major proportion.<sup>54-56</sup>

### 2a2. Reactivity

In metallocene-based pincer complexes of type A the metal M of the metallocene and the metal M' of the pincer fragment are relatively in close proximity, in fact the  $\text{M}\cdots\text{M}'$  length through space is approximately  $\sim 3.8 \text{ \AA}$ . This closeness produces a strong relationship between the redox potential of each metal.<sup>57, 58</sup> For example, Koridze and co-workers studied the redox potential of the ferrocene fragment in a series of  $\text{CpFePC}^{\text{Cp}}\text{PP}$ -pincer Pd(II) complexes (Scheme 3).<sup>57</sup> They found that variation of the P-substituent in  $\text{CpFePC}^{\text{Cp}}\text{PP-PdCl}$ , complexes **3**, did not produce a significant change in the redox potential of the respective Fe atoms. It is noteworthy that dimetallic species,  $\text{CpFePC}^{\text{Cp}}\text{PP-PdCl}$ , showed a slightly lower redox potential than its monometallic precursor,  $\text{CpFePCH}^{\text{Cp}}\text{PP}$ . A similar behavior was observed in ferrocene-based

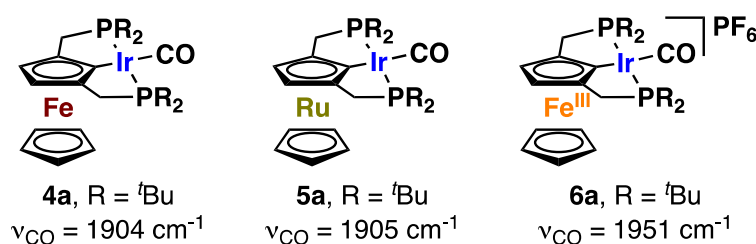
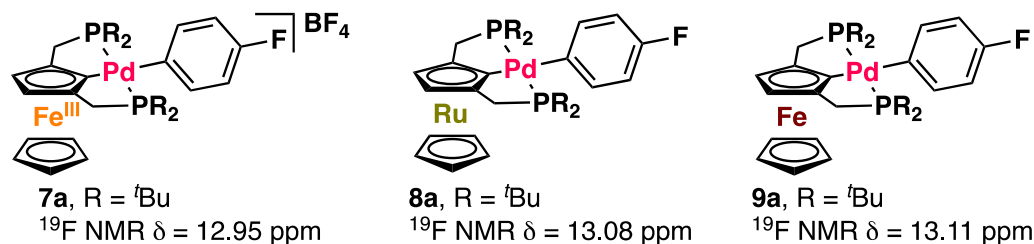
Pt(II)-pincer complexes, where the donor atoms of the pincer were N- and O-atoms instead of phosphines.<sup>58</sup>



**Scheme 3.** Redox potential of ferrocene-based pincer complexes.<sup>57</sup>

The electronic properties of the metallocene-based pincer complexes have been studied through infrared and NMR spectroscopy (Scheme 4).<sup>59, 60</sup> Koridze and co-workers prepared a series of carbonyl pincer complexes, CpMPC<sup>Cp</sup>P-IrCO (M=Fe, Ru, Fe<sup>III</sup>), and recorded their FT-IR spectra. They observed that the  $\nu$ CO stretching frequencies of the ruthenocene **5a** and ferrocene **4a** derivatives were very similar, 1905 and 1904  $\text{cm}^{-1}$ , respectively. Hence the authors concluded that the metal in the metallocene fragment does not produce significant changes in the electronic power of the pincer ligand. In contrast, when Fe(II) is oxidized to Fe(III), the  $\nu$ CO is shifted up to 1951  $\text{cm}^{-1}$  which suggests that the higher oxidation state of the iron in the metallocene fragment produces an important electron-withdrawing effect and lowers the electron donating power of the pincer ligand that is reflected by the lower  $\nu$ CO. Interestingly, in the near-infrared spectra of the Fe(III) derivative two broad and intense absorption bands at 10 000 and 7 000  $\text{cm}^{-1}$  were observed. These bands point to an intervalence transfer, thus an electron delocalization between metal centers occurs with a charge transfer from Fe to Ir. This implies a certain degree of *intermetallic* interaction.

The electronic properties of the metallocene-based pincer complexes can also be determined by NMR. For this purpose, Koridze and co-workers compared the <sup>19</sup>F chemical shift of a series of *p*-fluoro-phenylpalladium complexes, CpMPC<sup>Cp</sup>P-PdC<sub>6</sub>H<sub>4</sub>F-4 (M=Fe, Ru, Fe<sup>III</sup>) (Scheme 4).<sup>60</sup> Interestingly, the <sup>19</sup>F NMR data correlate with the corresponding  $\nu$ CO of Ir(I)-based analogues complexes. However, this approach shows some limitation, the main reason being the presence of paramagnetic species that may produce misleading results.

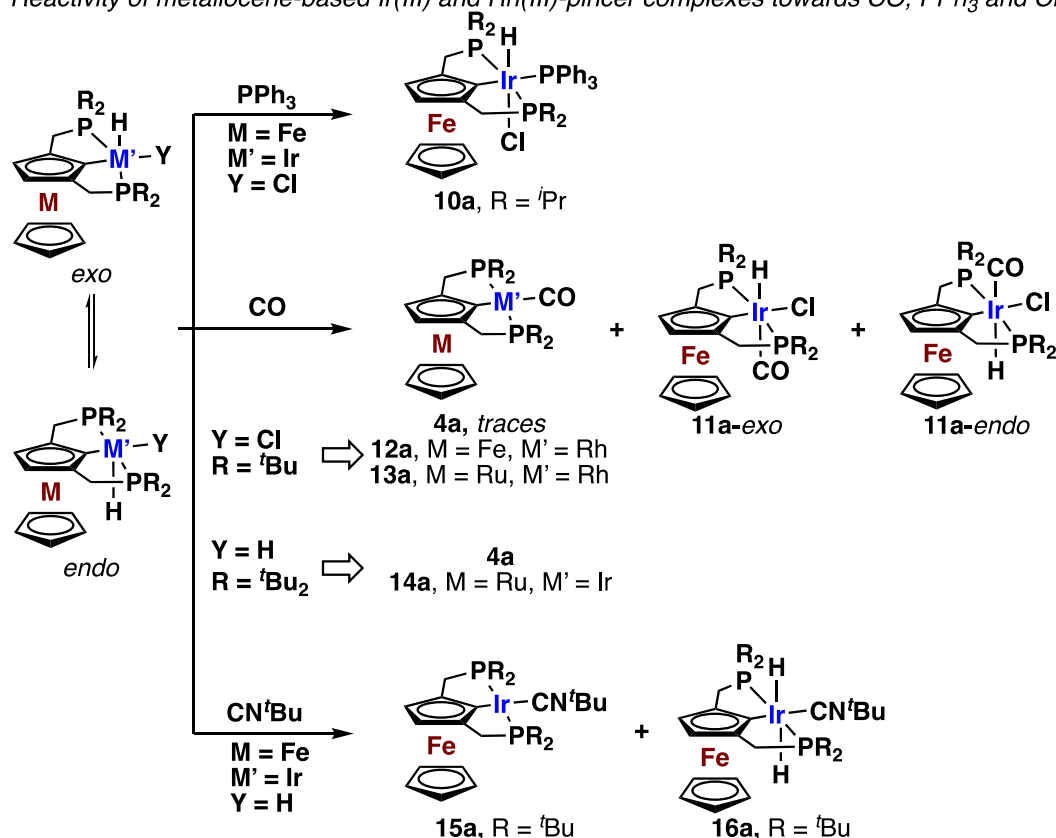
FT-IR of carbonyl Ir(I) complexes<sup>59</sup>View Article Online  
DOI: 10.1039/D1DT03870B<sup>19</sup>F NMR of fluoro-aryl Pd(II) complexes<sup>60</sup>

**Scheme 4.** Determination of electronic properties of the metallocene-based pincer ligands by FT-IR and <sup>19</sup>F NMR spectroscopy.

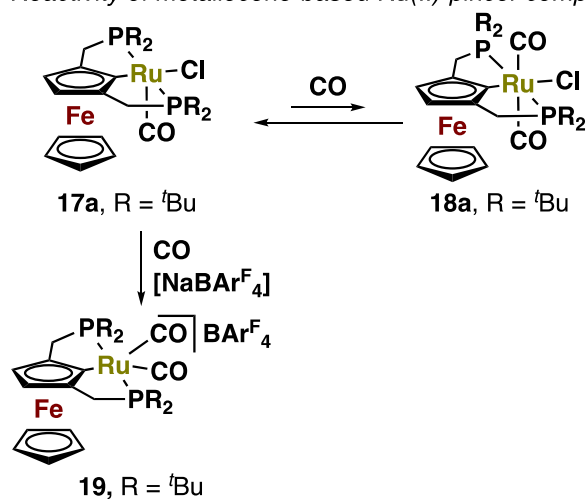
Common reactions that have been studied are both the oxidation of the metal M at the metallocene fragment and the reactions of the metallocene-pincer-metal complexes towards neutral ligands (Scheme 5). In some cases the Fe(II) atom in these compounds was oxidized to Fe(III) using [Fe(Cp)<sub>2</sub>]X (where X = PF<sub>6</sub> or BF<sub>4</sub>) or CF<sub>3</sub>SO<sub>3</sub>SiMe<sub>3</sub>.<sup>54, 55, 57, 58, 61</sup>

Examples of reactions of metallocene-based pincer complexes with neutral ligands are listed in Scheme 5. Koridze and co-workers described the reaction of *rac*-CpFePC<sup>Cp</sup>P-Ir(III)ClH with triphenylphosphine,<sup>62</sup> affording CpFePC<sup>Cp</sup>P-Ir(III)ClH(PPh<sub>3</sub>) (**10a**), in which the hydride ligand is *cis* to the triphenylphosphine ligand. This stereochemistry is in agreement with the observation of two <sup>2</sup>J<sub>H,P</sub> coupling constants for the hydride ligand (<sup>2</sup>J<sub>H,P(Ph<sub>3</sub>)</sub> = 10.0 and <sup>2</sup>J<sub>H,P(iPr<sub>2</sub>)</sub> = 14.0 Hz). In the case of the corresponding ruthenocene analogue, they observed an *endo-exo* interconversion, the *endo:exo* ratio after heating at 90 °C being ~1:2 and ~1:5 after 9 h, respectively. Notably, reaction of *rac*-CpFePC<sup>Cp</sup>P-Ir(III)ClH with CO afforded a mixture of three compounds: two isomers **11** (*endo* and *exo*), and an Ir(I)-pincer complex **4a**.<sup>59</sup> The ratio of isomers was maintained during the reaction, the *endo*-isomer being the less abundant one. The Ir(I)-pincer derivative **4a** was present in a small amount. The latter species can be prepared independently and isolated in high yield starting from the dihydride species because the Ir(III) species formed undergoes a facile reductive elimination of H<sub>2</sub> in the presence of CO. A similar behavior is observed in the presence of CN<sup>t</sup>Bu, but in this case the reduction of Ir(III) is not complete, affording a ~3:1 mixture of two new complexes: an Ir(III)H<sub>2</sub>(CN<sup>t</sup>Bu) complex **16a**, and an Ir(I)CN<sup>t</sup>Bu complex **15a**. Using the corresponding Rh(III) analogues, the reaction with CO likewise afforded reduction to the corresponding Rh(I)CO species.<sup>63</sup> Reaction of CO with the ruthenium-pincer analogue **17a** initially generates an octahedral Ru(II)(CO)<sub>2</sub> species **18a**, but this species is unstable and undergoes rapid loss of one CO ligand.<sup>54, 55</sup> When the reaction is carried out in the presence of [NaBAR<sub>4</sub><sup>F</sup>] and CO, a Cl/CO exchange is observed, see Scheme 5.

Reactivity of metallocene-based Ir(III) and Rh(III)-pincer complexes towards CO, PPh<sub>3</sub> and CN<sup>t</sup>Bu.<sup>59, 62, 63</sup>



Reactivity of metallocene-based Ru(II)-pincer complexes towards CO.<sup>54, 55</sup>

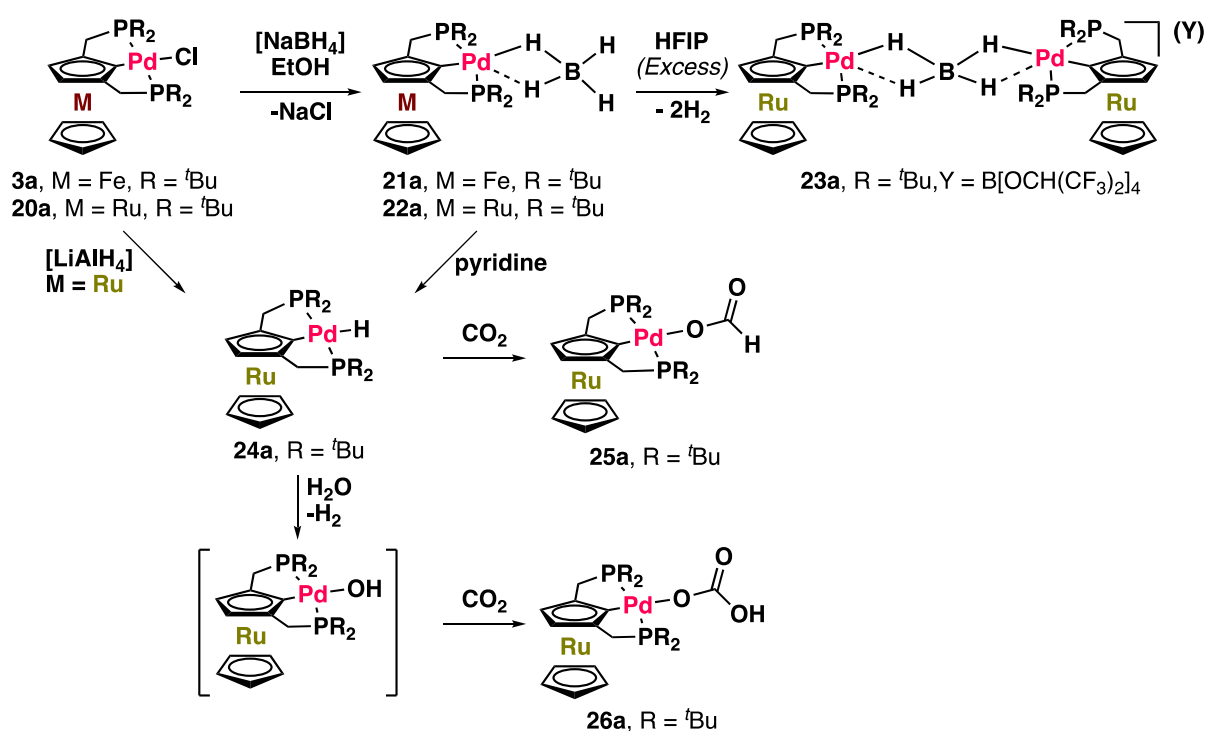


**Scheme 5.** Reactivity of metallocene-based pincer complexes towards PPh<sub>3</sub>, CO and CN<sup>t</sup>Bu.

The reaction of metallocene-based Pd(II)-pincer complexes (M = Fe (**3a**), Ru (**20a**)) with [NaBH<sub>4</sub>] in refluxing ethanol produced a ligand exchange between the chloride and the BH<sub>4</sub><sup>-</sup> anions, the latter anion being bonded to Pd in a rarely encountered η<sup>1</sup>-fashion (Scheme 6).<sup>57, 64, 65</sup> The molecular structure of CpFePC<sup>Cp</sup>P-PdHBH<sub>3</sub>, **21a**, in the solid state was elucidated by X-ray diffraction analysis.<sup>64</sup> Attempts to abstract the BH<sub>4</sub><sup>-</sup> anion with NH<sub>3</sub> were unsuccessful, whereas CpMPC<sup>Cp</sup>P-PdHBH<sub>3</sub> complexes on storage in CHCl<sub>3</sub> solution, gradually transformed

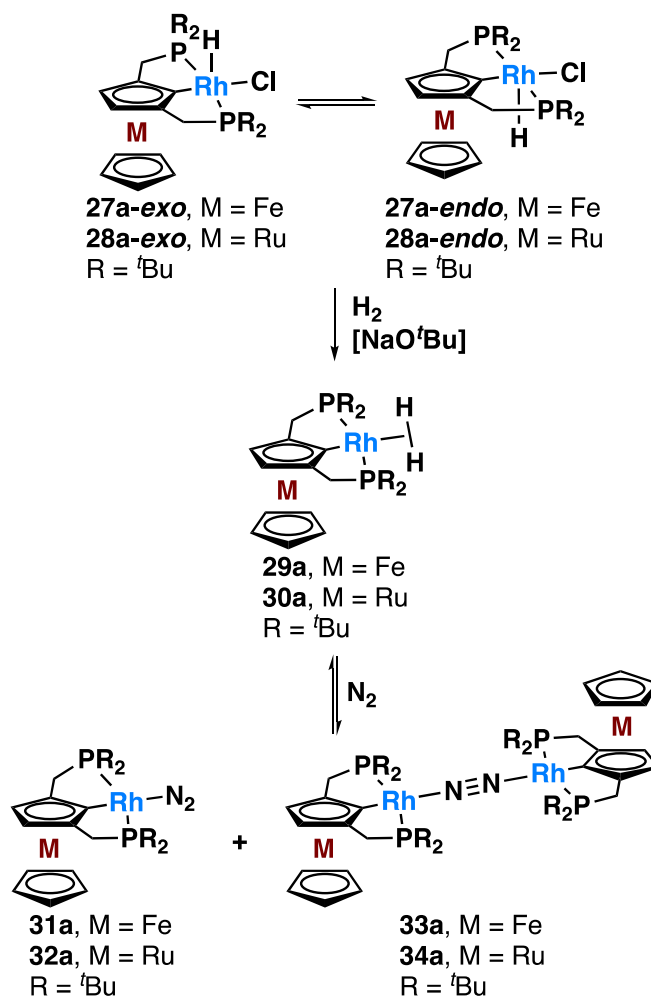


into the starting CpMPC<sup>Cp</sup>P-PdCl complexes. The CpRuPC<sup>Cp</sup>P-PdHBH<sub>3</sub> species **22a** react with very acidic alcohols, such as hexafluoro-*iso*-propanol (HFIP), to form species **23a** comprising two CpRuPC<sup>Cp</sup>P-Pd-cations bridge bonded by a η<sup>1</sup>,η<sup>1</sup>-HBH<sub>2</sub>H-anion *via* a proton transfer with H<sub>2</sub> release.<sup>66</sup> The CpRuPC<sup>Cp</sup>P-PdHBH<sub>3</sub> species **22a** reacts with pyridine to afford a monohydride compound **24a**. The latter complex can also be obtained by reaction of CpRuPC<sup>Cp</sup>P-PdCl, **20a**, with [LiAlH<sub>4</sub>] instead of [NaBH<sub>4</sub>] in high yields. Finally, CpRuPC<sup>Cp</sup>P-PdH is highly reactive toward CO<sub>2</sub>, forming a formate complex **25a**; in the presence of H<sub>2</sub>O the final product is a hydrocarbonate Pd(II) complex **26a**.



**Scheme 6.** Reactivity of metallocene-based Pd(II)-pincer complexes.<sup>57, 64-66</sup>

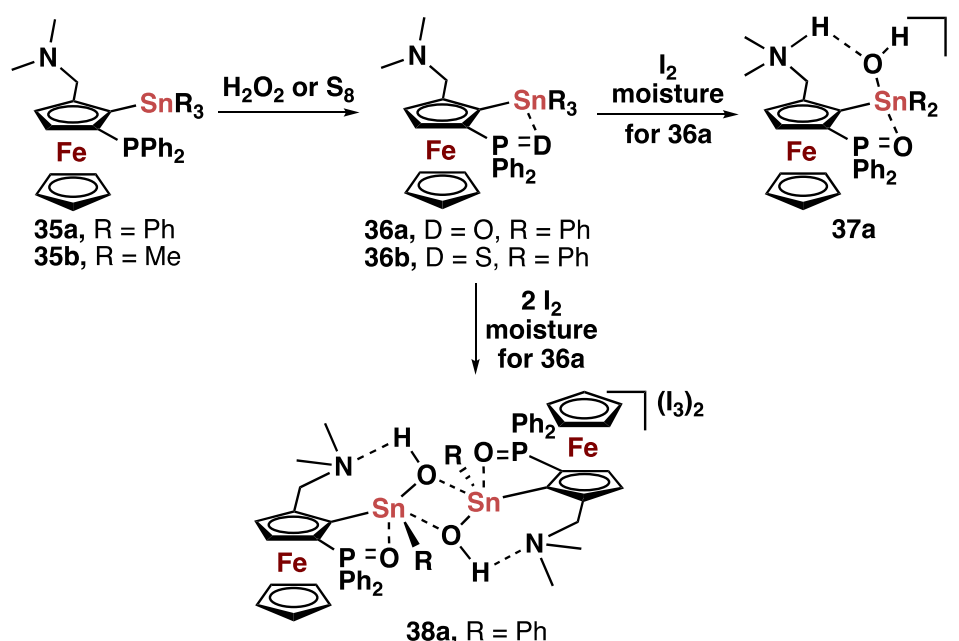
In 2019 Polezhaev described the synthesis of CpMPC<sup>Cp</sup>P-RhClH, see also Scheme 2b, and the exchange of the hydride and chlorine ligand by a dihydrogen molecule in the presence of [NaO<sup>t</sup>Bu] (Scheme 7).<sup>63</sup> The reaction was carried out under an hydrogen atmosphere. Unexpected was the fact that the dihydrogen ligand could be exchanged by N<sub>2</sub>, affording a mixture of dinuclear and mononuclear Rh(I) species. These novel complexes could be key for the development of a new type of (de)-hydrogenation catalysts.



**Scheme 7.** Reactivity of ferrocene-based Rh(I)-pincer complexes towards  $\text{H}_2$  and  $\text{N}_2$ .<sup>63</sup>

In 2019 Jurkschat and co-workers explored the reactivity of iron-tin(IV) complexes using a ferrocene moiety carrying on one of its Cp-rings a  $\text{NC}^{\text{Cp}}\text{P}$ -pincer type scaffold (Scheme 8).<sup>67</sup> The molecular structure of the  $\text{CpFeNC}^{\text{Cp}}\text{P-SnR}_3$  tetraorganotin(IV) complexes, **35a** and **35b**, confirmed that instead of a  $\text{N,C}^{\text{Cp}},\text{P}$ -terdentate binding the scaffold acted as a  $\text{C}^{\text{Cp}}$ -monodentate ligand with free, dangling  $\text{CH}_2\text{NMe}_2$  and  $\text{P(X)R}_2$  groupings. In the triphenyl and trimethyltin derivatives, the  $\text{P}\cdots\text{Sn}$  were 3.6146(7) and 3.8730(8), respectively. Likewise, the  $\text{N}\cdots\text{Sn}$  distances were 3.6146(7) and 3.257(2) Å, respectively. In spite of the fact that in both complexes the  $\text{P}\cdots\text{Sn}$  distances are shorter than the sums of the van der Waals radii of the corresponding atoms substantial  $\text{P}\cdots\text{Sn}$  interaction can be excluded. However, the fact that in both compounds the orientation of the respective N donor atoms are pointing to the Sn center trans to C(Ph) in **35a** to C(Me) the Sn atom can be seen as [4+1]-coordinated with a N atom.<sup>67</sup> The  $\text{N}\cdots\text{Sn}$  interaction is suitable to form a five-membered chelate ring, and consequently be entropically stabilized. In contrast, the  $\text{P}\cdots\text{Sn}$  interaction may form a non-stabilize four-membered chelate ring.

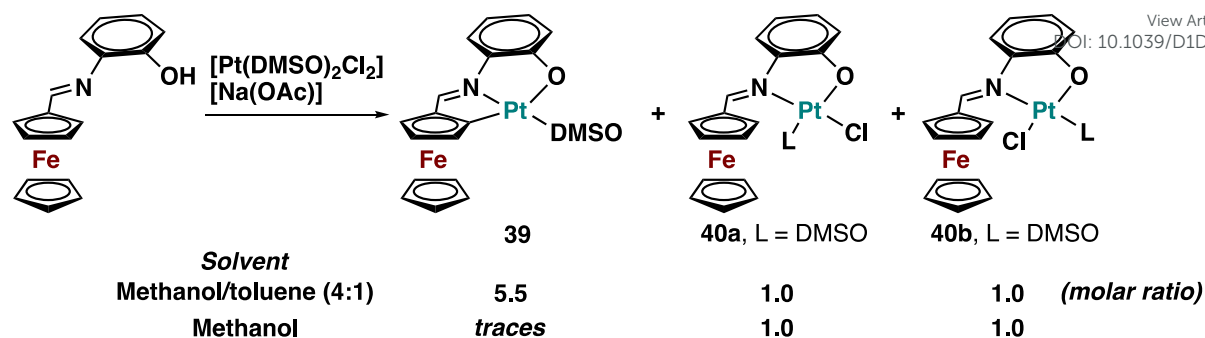
Oxidation of the phosphine atom with  $\text{H}_2\text{O}_2$  or  $\text{S}_8$ , affords the corresponding  $\text{P}=\text{O}$  and  $\text{P}=\text{S}$  complexes which extends coordination *via* a 4-membered chelate ring *via*  $\text{P}-\text{Sn}$  in **35** to a 5-membered one in **36**. Tendency to forming a  $\text{Sn}\cdots\text{O}$  or  $\text{Sn}\cdots\text{S}$  interaction are shown indeed, distances were 2.791(2) and 3.545(2) Å, respectively, again shorter than the sum of the van der Waals radii of the respective atoms. Interestingly, the  $\text{Sn}\cdots\text{O}$  distance is shorter than the one found in the symmetrical  $(\text{PO})\text{C}(\text{PO})$  tin complexes (3.353(3) and 3.355(3) Å).<sup>68</sup> In contrast, the  $\text{Sn}\cdots\text{N}$  distances were considerably longer, being 3.883(3) Å for **36a** and 3.626(2) Å for **36b** indicating that there is no significant intramolecular  $\text{Sn}\cdots\text{N}$  interaction. The addition of  $\text{I}_2$  and moisture to **36** afforded—resulted in the formation of pseudo-pincer complexes by the presence of a hydrogen bond between the  $(\text{Sn})\text{OH}$  ligand and the nitrogen atom. Pseudo-pincer complexes have been previously described and are formed by a non-covalent interaction of one arm of the “pincer” ligand with a ligand on the metal center.<sup>69</sup>



**Scheme 8.** Reactivity of ferrocene-based Sn complexes with a pincer type scaffold.<sup>67</sup>

### 2b1. Metallocene-based pincer-metal complexes of type A'

López and co-workers prepared a ferrocenyl Schiff base by the condensation of ferrocene-carboxaldehyde and 1-aminophenol (Scheme 9).<sup>58, 70</sup> The Schiff base was then reacted with  $[\text{PtCl}_2(\text{DMSO})_2]$  in the presence of  $[\text{Na}(\text{OAc})]$ . They observed that when using methanol, a mixture of complexes was obtained, while *ortho*-cyclometallation hardly occurred. In contrast, using a toluene/methanol (4:1) mixture, the formation of an *ortho*-metallated *C,N,O*-pincer complex **39** was observed as the major product. Although, formally, in **39** the three donor atoms, in a  $\text{C}^{\text{Cp}}\text{N}^{\text{imine}}\text{O}^{\text{phenol}}$  arrangement, are in one plane and the pincer manifold is covalently bonded to the metallocene-Fe atom and the Pt(II) atom in the dianionic C,N,O-manifold that is a very flexible one and is in kinetic sense less rigidly organized.

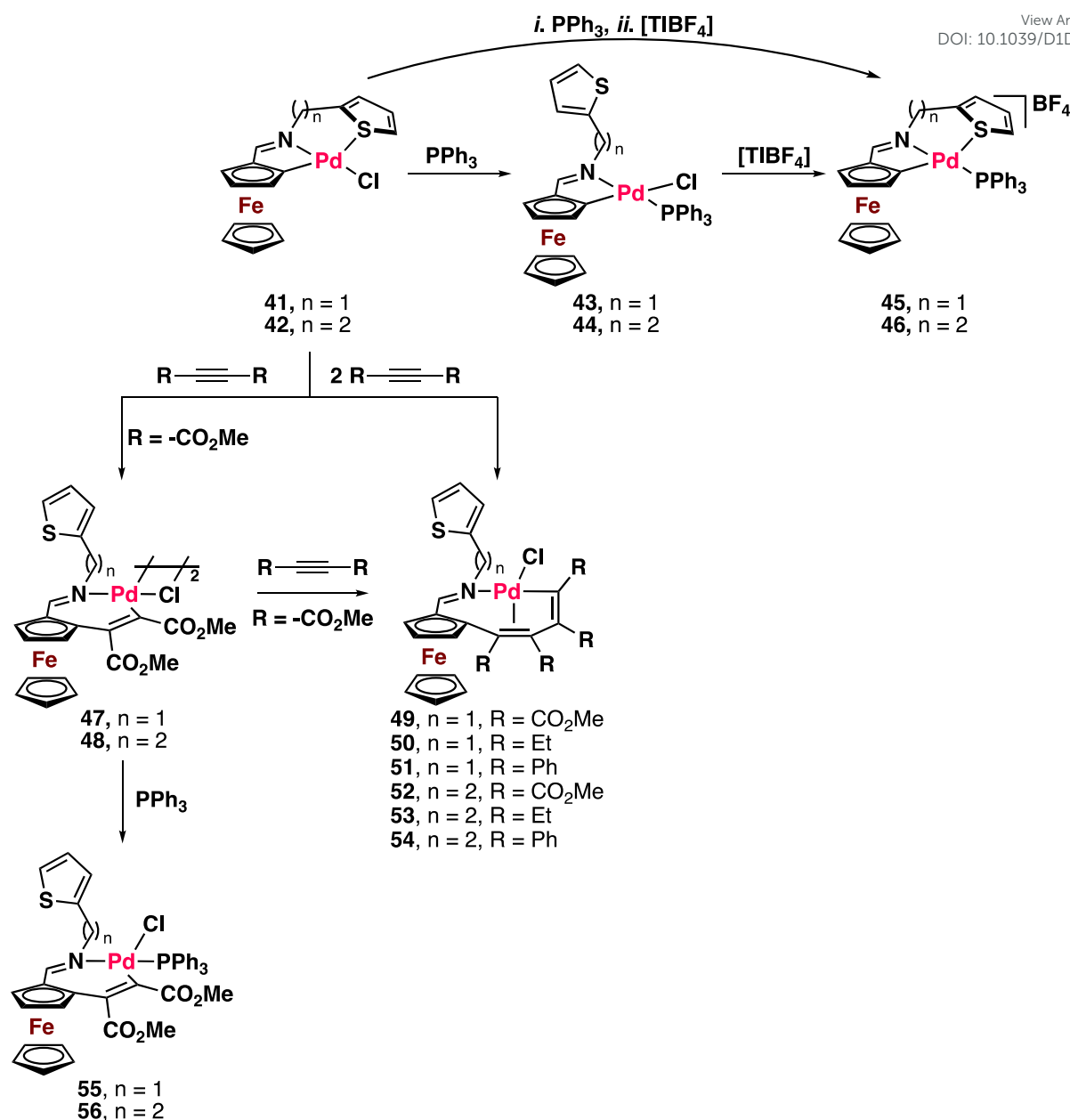


**Scheme 9.** Reaction of a ferrocenyl Schiff base with  $[\text{PtCl}_2(\text{DMSO})_2]$  in various solvent mixtures. In methanol exclusively the *cis*- and *trans*-Cl, O-Pt(II) coordination compounds **40** are formed whereas in a 4:1 MeOH/toluene mixture *ortho*-cyclometallation occurs with formation of the ferrocenyl-Pt(II)-*cis*-pincer complex **39**. It must be noted that in **39** the pincer platform is different from the  $\text{CpMPC}^{\text{Cp}}\text{P-M}^{\text{L}}\text{L}_n$  discussed above, see text.<sup>58</sup>

### 2b2. Reactivity.

In 2010 López and co-workers reported the synthesis of a series of Schiff bases bearing a thiophene group, instead of the phenoxy-O donor anion in **39**, and then synthesized the Pd(II) derivatives by reacting the pincer ligand precursor with  $[\text{Na}_2\text{PdCl}_4]$  in the presence of sodium acetate (Scheme 10).<sup>71</sup> The pincer motif in these complexes is monoanionic and primarily consisting of a monoanionic,  $\text{C}^{\text{Cp}}\text{N}^{\text{imine}}$  bidentate-bonded ferrocenyl unit with potentially, *i.e.* depending on the tether-length between  $\text{N}^{\text{imine}}$  and  $\text{S}^{\text{thiophene}}$ , an additional S-Pd interaction. This latter interaction then installs the pincer motif, which, however, is kinetically instable and flexible.

Interestingly, the addition of triphenylphosphine to the metallocene-based pincer complexes **41** and **42** produced the resulted in de-coordination of the thiophene ligand, and the coordination of the triphenylphosphine. This suggested that cyclic thioethers form relatively labile Pd-S bonds. Furthermore, the exchange of the chloride by triphenylphosphine was achieved by the addition of a strong halogen scavenger ( $\text{TIBF}_4$ ). Two years later, they explored the reactivity of the ferrocene-based Pd(II)-pincer complexes towards alkynes (Scheme 10).<sup>72</sup> Interestingly, the pincer-Pd bond undergoes an insertion reaction of the alkyne, probably favored by the lability of the thiophene-S-Pd interaction. If an excess of the alkyne is present, a double insertion of alkyne occurs, producing a final complex with C-Pd  $\sigma$ - and  $\pi$ -bonds. The double insertion also depends on the nature of the substituents on the alkyne. Electron-donating groups favored the double insertion, while using electron-withdrawing group, the mono-insertion product can be isolated. This approach has been extensively studied by Pfeffer *et al.* for the reaction of, for example,  $\text{PdCl}(\text{C}_6\text{H}_4\text{CH}_2\text{NMe}_2)_2$  dimer with different alkynes.<sup>73-83</sup> The insertion of alkynes into the non-metallocene based complexes is controlled by steric rather than electronic factors.<sup>82</sup>

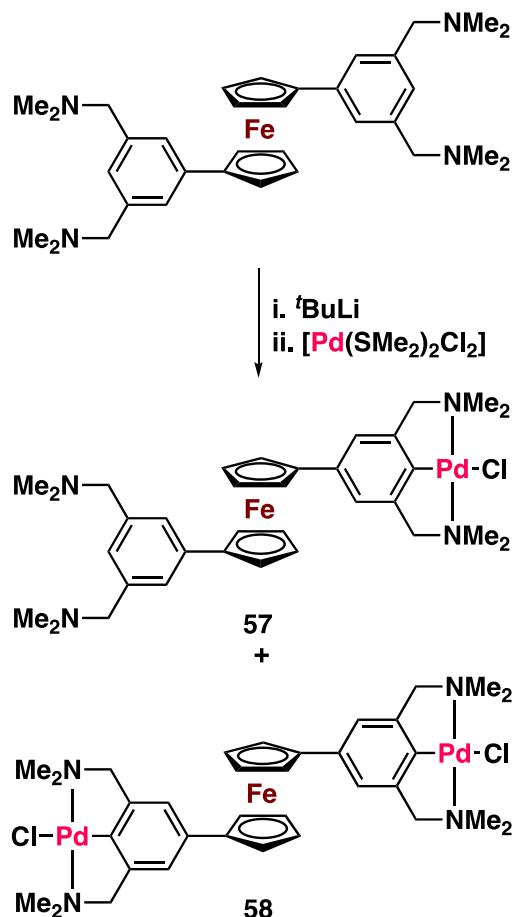


**Scheme 10.** Ferrocenyl Schiff base complexes,  $\text{CpFeN}^{\text{Imine}}\text{C}^{\text{CpS}^{\text{Thiophene}}}\text{-PdCl}$ , and their reactivity with alkynes.<sup>71, 72</sup>

### 2c1. Metallocene-based pincer complexes of the type **B**

In 2003, van Koten and coworkers reported the first example of metallocene-based pincer complexes of the type **B** (Scheme 11).<sup>84</sup> In these complexes the metallocene entity is *para*-bonded to the aryl ring of the pincer- $\text{ML}_n$  unit. Consequently, electronic communication between the Fe and Pd center is occurring by a combination of mesomeric and inductive effects exerted by the *para*-substituent effect of the  $\text{CpFeC}_5\text{H}_4$ -grouping. Conversely, the PdCl unit through the arene's *para*-C  $\pi$  and  $\sigma$  effects affects the metallocene's properties, *vide infra*.<sup>85</sup> The synthesis of those compounds was achieved in two steps. First, reaction of the arene precursor  $\text{Fe}[\eta^5\text{-C}_5\text{H}_4(\text{NCNH})]_2$  with two equivalents of  $t\text{BuLi}$  yielded a mixture of the corresponding mono- and di-lithiated products. Subsequent transmetalation with  $[(\text{Me}_2\text{S})_2\text{PdCl}_2]$  afforded a mixture of the mono- and bis-palladated compounds **57** and **58**,

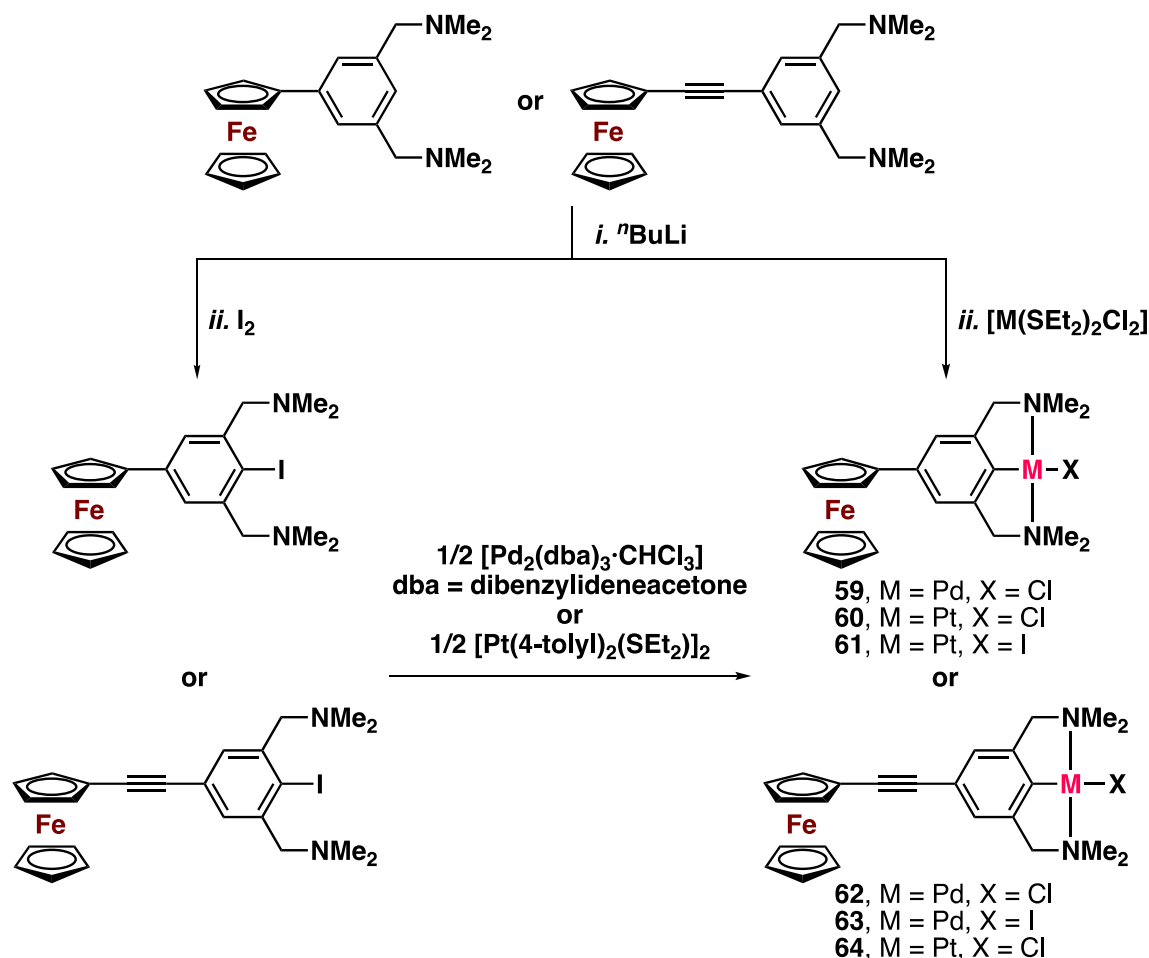
respectively. Cyclic voltammetry data revealed that the iron fragment in these multimetallic complexes is easily oxidized because the PdCl moieties can act as electron releasing substituent, vide infra Scheme 19.<sup>86</sup> The Fe(II)/Fe(III) oxidation potential for the monometallic specie was 0.03 V, while for complex **58** was -0.03 V.



**Scheme 11.** Synthesis of metallocene-substituted NCN arylpincer-Pd(II) complexes (type **B**).<sup>84</sup>

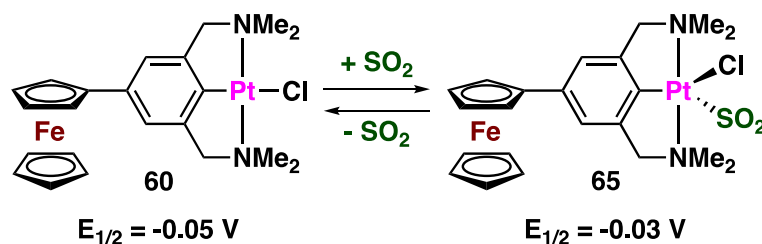
The set of metallocene-based pincer complexes of type **B** was expanded following two synthetic approaches. Two different methodologies were followed to obtain the respective  $\text{CpFeC}_5\text{H}_4(\text{CC})_n(\text{NCN})\text{Pd}(\text{II})\text{Cl}$  or  $\text{Pt}(\text{II})\text{Cl}$  ( $n = 0$  or  $1$ ) derivatives, see (Scheme 12).<sup>87, 88</sup> The first strategy comprised reaction of the metallocene-pincer precursor with  $t\text{BuLi}$  followed by a transmetalation reaction. The second strategy involved the synthesis of the iodide precursor from the organolithium complex. Subsequently, using a low valent Pd or Pt precursor,  $[\text{Pd}_2(\text{dba})_3 \cdot \text{CHCl}_3]$  or  $[\text{Pt}(4\text{-tolyl})_2(\text{SEt}_2)]_2$ ,<sup>89, 90</sup> respectively, oxidative addition of the C-I bond afforded the corresponding Pd and Pt derivatives. Interestingly, the presence of the alkyne linker, between the metallocene and the pincer fragment, produced the bimetallic species in a considerably lower yield as compared with the bimetallic one lacking this linker. Likewise, cyclic voltammetry experiments revealed that the presence of the alkyne group produces a shift of the Fe(II)/Fe(III) redox potential to more positive values, which most likely is due to the electron-withdrawing character of the triple bond. Interestingly, coordination of palladium (**62**, **63**) or platinum (**64**), cf., produced a slight shift to negative potential values in comparison with the free pincer ligand precursors. A similar behavior was described by Lang and co-workers

for bis(ferrocene)-bis(pincer) and mono(ferrocene)-bis(pincer) complexes derived from Pd(II) and Pt(II).<sup>91, 92</sup>



**Scheme 12.** Synthesis of ferrocene-based Pd(II) and Pt(II)-pincer complexes.<sup>87</sup>

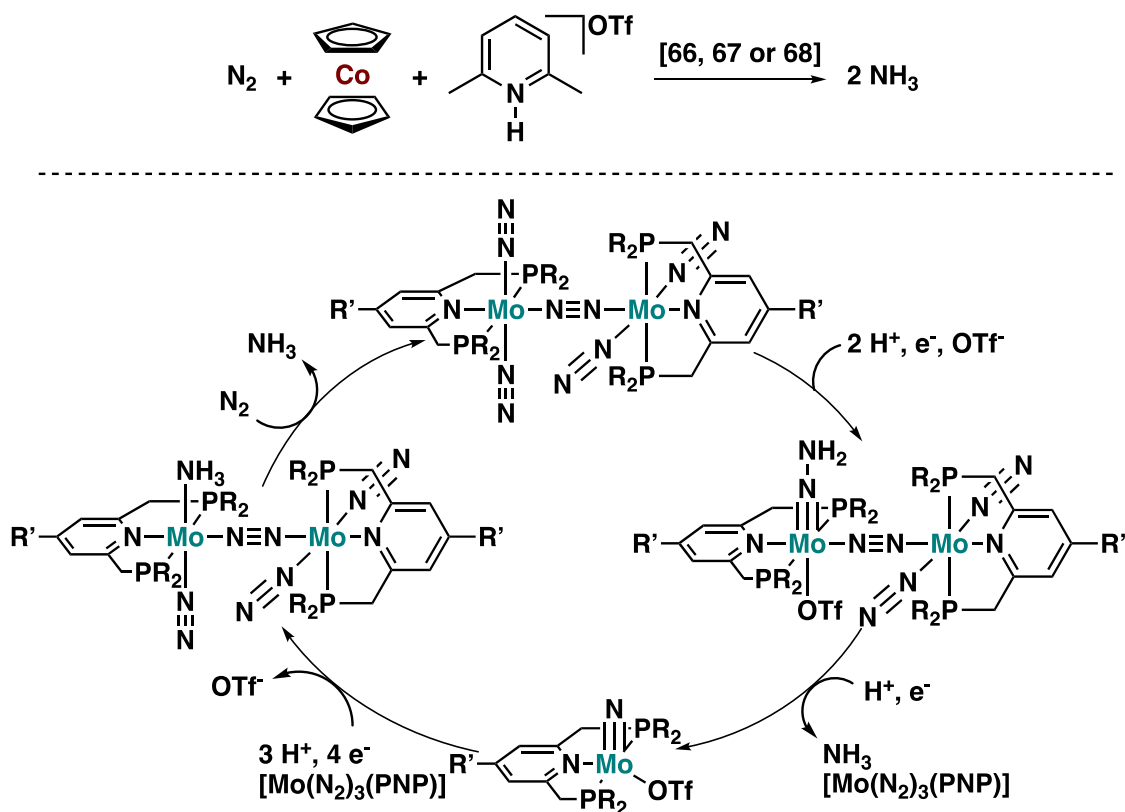
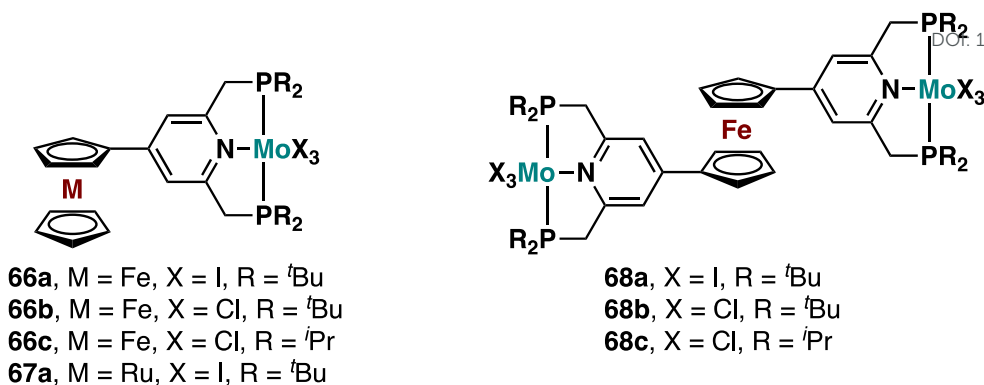
The reversible  $\eta^1$ -bonding of  $\text{SO}_2$  to the Pt center of NCN-pincer platinum complexes, involving interaction of the filled  $d_z^2$ -Pt orbital (acting as an L-type ligand) into the empty  $\sigma^*$ - $\text{SO}_2$  one, is notable because it produces a color exchange from colorless to orange.<sup>93-97</sup> Electrochemical properties of the  $\text{SO}_2$ -coordinated (**65**) and the  $\text{SO}_2$ -free compound (**60**) in solution were studied showing the different redox potentials of Fe(II) in the  $\text{SO}_2$ -coordinated and  $\text{SO}_2$  free state (Scheme 13).<sup>87</sup> These observations, both by colorimetric and voltametric analysis, revealed that the reduced electron density on Pt(II), caused by the  $\text{SO}_2$  coordination, is relayed to the Fe atom of the ferrocene, thus causing a decrease of the Fe redox potential.



**Scheme 13.**  $\eta^1$ -Coordination of SO<sub>2</sub> (filled  $d_z^2$ -Pt orbital into the empty  $\sigma^*$ -SO<sub>2</sub>) to the Pt(II) center of ferrocene-based Pt(II)-pincer complex **60**.<sup>87</sup>

Recently, Yoshizawa and Nishibayashi reported the synthesis of a series of metallocene mono- and bis-(PNP-pincer molybdenum) derivatives carrying one or two PNP-pincer ligands of which all three coordinating sites are neutral two-electron donors.<sup>98-100</sup> The reactions of both the metallocene-mono-PNP- and di-PNP-pincer ligands with [MoX<sub>3</sub>(THF)<sub>3</sub>] afforded the desired complexes in good yields, see Scheme 14. These CpMC<sub>5</sub>H<sub>4</sub>-PNP-pincerMoX<sub>3</sub> and M(C<sub>5</sub>H<sub>4</sub>-PNP-pincerMoX<sub>3</sub>)<sub>2</sub> complexes (**66**, **67** and **68**) showed excellent reactivity towards molecular dinitrogen. Notably, the reaction of these metallocene-PNP-pincer Mo(III) complexes in the presence of Na-Hg under N<sub>2</sub> afforded dinitrogen-bridged dimolybdenum-dinitrogen complexes.<sup>101-103</sup> In the presence of cobaltocene and 2,6-lutidinium triflate ([LutH](OTf)) these complexes are catalysts for the transformation of N<sub>2</sub> into NH<sub>3</sub>. The proposed catalytic cycle, involving electron and proton transfer, is shown in Scheme 14. In 2015, Yoshizawa described that merger of a ferrocene fragment with the PNP-pincer Mo fragment enhanced the catalytic activity of the Fe-Mo catalyst, indeed, by accelerating the reduction steps, as a result of electron transfer from the Fe atom in the ferrocene to the Mo atom in the pincer ligand.<sup>98, 100</sup> In fact, the occurrence of such interaction was confirmed by electrochemical and theoretical studies. Likewise, the catalytic reaction can be accelerated by the presence of electron-donating groups such as -OMe at the aryl-pincer *core*, thus promoting the protonation step of the coordinated N<sub>2</sub> ligand. It is worth to note that the ferrocene-bis(PNP-pincer Mo) derivatives showed lower activity than their mono-metallic analogues.

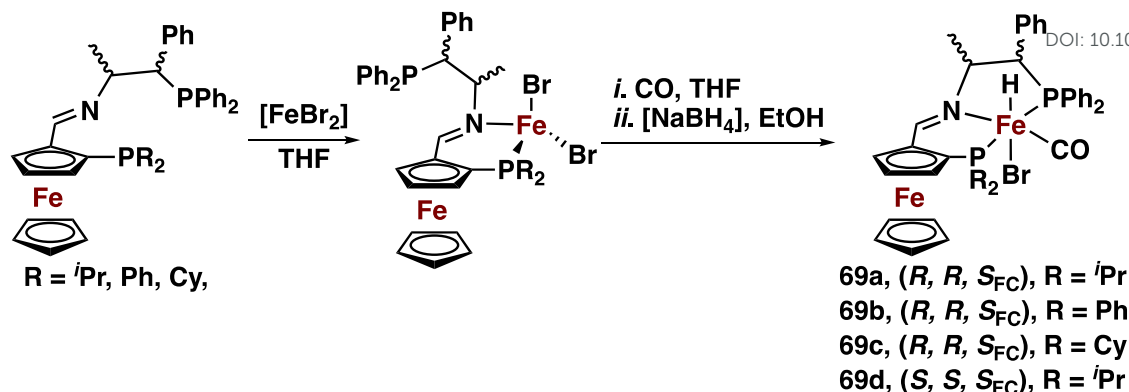




**Scheme 14.** Synthesis of  $\text{NH}_3$  from  $\text{N}_2$  catalyzed by metallocene-based Mo-pincer complexes.<sup>98-100</sup>

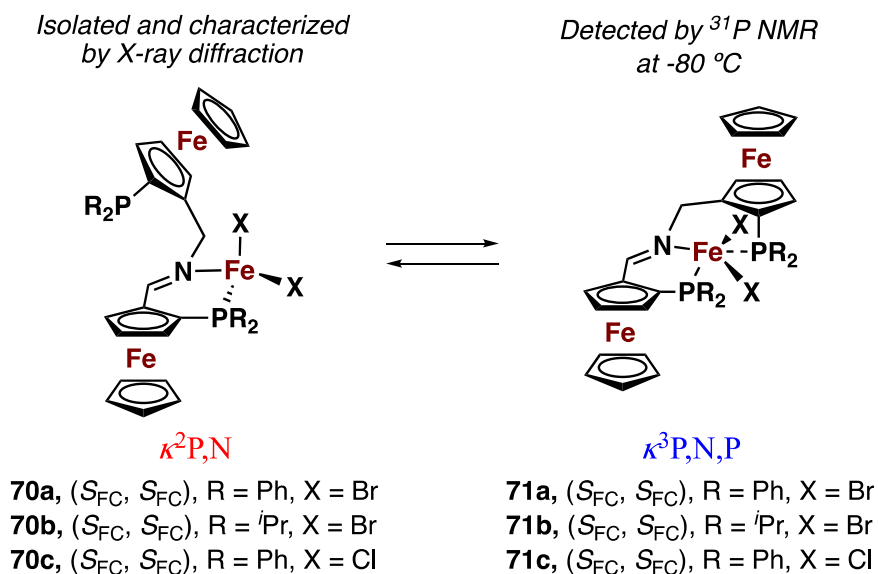
### 2d1. Metallocene-based pincer complexes of the type C

In the literature, there are few examples of complexes of type C.<sup>104-108</sup> The bimetallic compounds consist of a ferrocene moiety, that contains on one of its Cp rings a set of *ortho* positioned substituents that can function as ligands to a second metal center, *i.e.*, a  $\text{N}^{\text{imine}}$ , P bidentate ligand and a monodentate  $\text{P}'$  ligand.<sup>104</sup> When all three donor sites coordinate to a second metal site a neutral pincer-type manifold is created, see Scheme 15. In this structure the cyclopene-1,2-diyl element is placed in a bridge between two of the donor atoms. Consequently, it is worthy to note that although the metallocene and a pincer type fragment are present, communication between the two metal centers will be absent or very weak.



**Scheme 15.** Synthesis of ferrocene-based (*P,N*)*P'*-coordinating pincer-Fe(II)Br(CO)H complexes.<sup>104</sup>

However, it is obvious that because of the planar chirality in combination with the fact that the substituents at the Cp ring are different, these compounds exist as a complex set of stereoisomers. Zirakzadeh and co-workers reported the two-step synthesis of ferrocene-based Fe(II)-pincer complexes.<sup>104</sup> First, the *rac*-CpFeC<sub>5</sub>H<sub>3</sub>(*P,N*)*P'*-ligand is reacted with anhydrous FeBr<sub>2</sub> which yields a *P,N*-bidentate coordinated *rac*-CpFeC<sub>5</sub>H<sub>3</sub>(*P,N*)*P'*FeBr<sub>2</sub> complex. Subsequent exposure of the latter complex to CO (1 atm), followed by the addition of NaBH<sub>4</sub> yielded the corresponding *rac*-iron hydride compounds in which the (*P,N*)*P'* manifold is bonded as a  $\kappa^3$ -(*P,N*)*P'* tridentate coordinated pincer motif.



**Scheme 16.** Different coordination modes of a  $\kappa^2$ -(*P,N*) and  $\kappa^3$ -(*P,N*)*P'* ligand.<sup>105</sup>

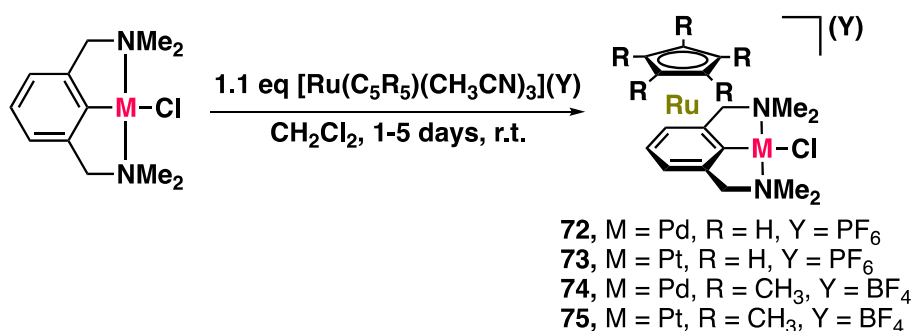
It is noteworthy that the (*P,N*)*P'*-pincer ligands in **69** contain a five- and a six-membered chelate ring having the central N-Fe coordination bond in common. When the five-membered ring is extended to a six-membered one, see Scheme 16, only the *P,N*-chelate product is formed in the solid state.

Temperature dependent <sup>31</sup>P NMR experiments revealed that in solution *P'* behaves as a dangling ligand; at low temperature (-80 °C) *P'*-Fe coordination is observed whereas at higher

temperatures it is present as a free donor site. Consequently, these complexes exist in solution as an equilibrium between  $\kappa^2$ -(*P,N*)- and  $\kappa^3$ -(*P,N*)*P'*-bound species (Scheme 16).<sup>105</sup>

### 2e1. Metallocene-pincer metal sandwich compounds

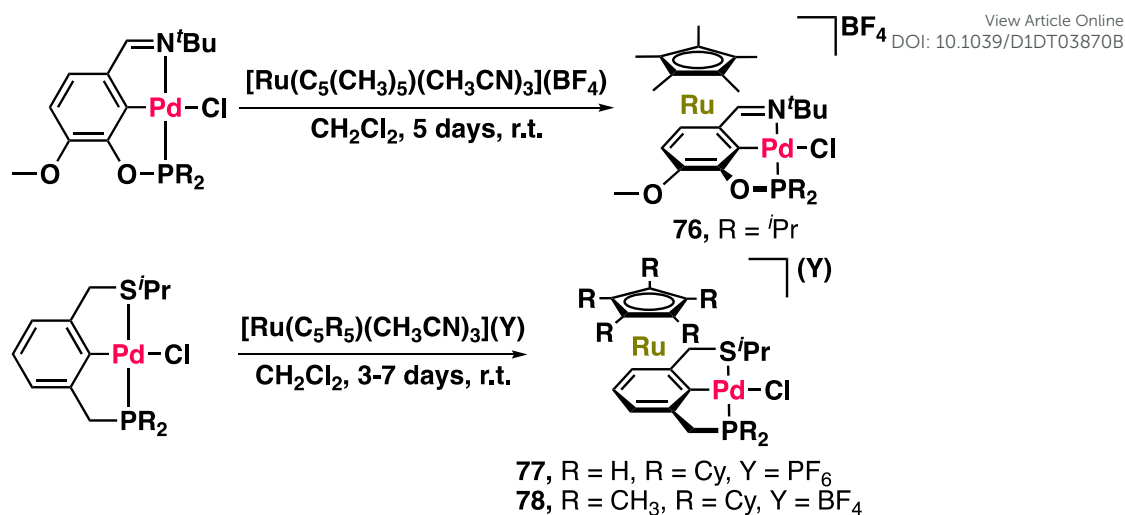
An obvious extension of the ways to merge a metallocene with a pincer-metal complex, see the series **A-C** in Scheme 1, is to combine a half sandwich type complex, *e.g.* arenophiles  $[\text{CpRu}]^+$  and  $[\text{Cp}^*\text{Ru}]^+$ , with the pincer metal complex, *i.e.*, making use of the  $\eta^6$ -binding of arene pincer's  $\pi$  system to a half sandwich CpM-cation. The first example of this approach, reported by Bonnet et al,<sup>86</sup> is shown in Scheme 17. This approach has great flexibility and is applicable for the many examples of pincer-metal complexes containing an arene derived carbo-anion.<sup>109-114</sup>



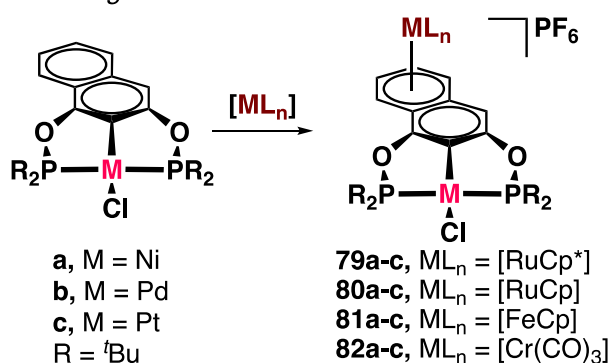
**Scheme 17.** First examples of metallocene-pincer metal sandwich compounds.<sup>86</sup>

When a parent pincer metal complex is used, in which the two flanking donor sites are different, an aryl-pincer-M' complex with planar chirality is created. Coordination of the arenophilic CpM-cation to pincer's  $\pi$  system then affords diastereomeric compounds, see Scheme 18.<sup>109</sup>

115



b. Le Lagadec<sup>115</sup>

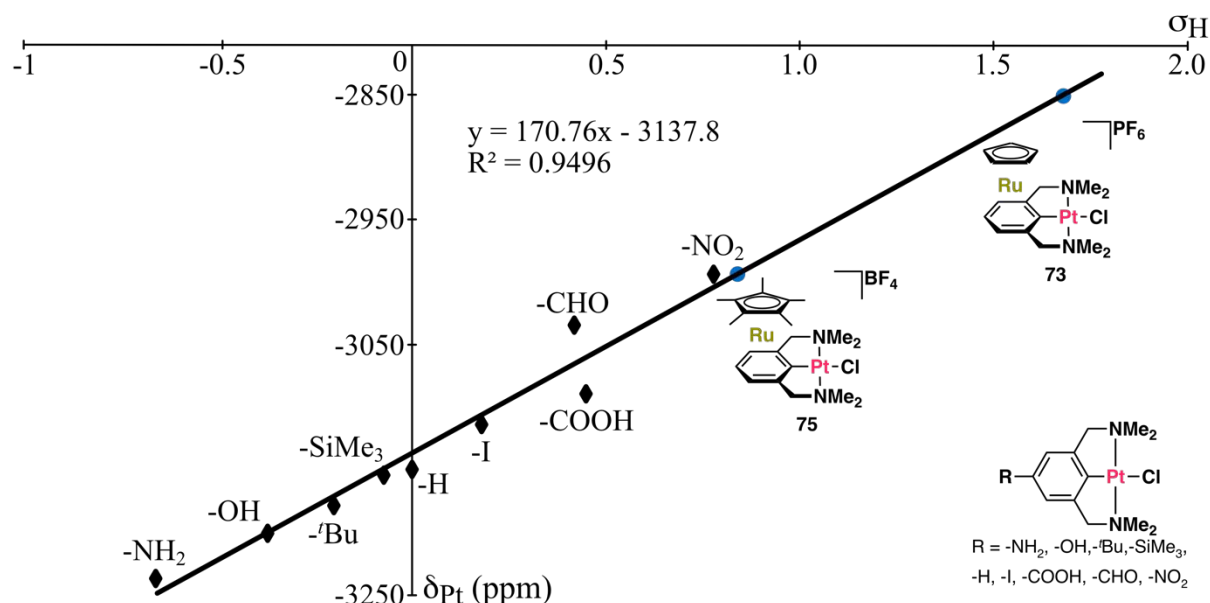


**Scheme 18.** Synthesis of heterobimetallic sandwich-type complexes *via* a direct route involving coordination of the arenophilic CpM'-cation directly to pincer's  $\pi$  system of a pre-made pincer-metal complex. Two easy ways are shown how to create diastereomeric metallocene-pincer metal sandwich compounds starting from planar chiral pincer-M' moieties; a) by using different flanking donor arms and b) starting from an unsymmetrically substituted arene ring system.

The formation and presence of the diastereoisomeric compounds could be established in solution by NMR using the enantiomerically pure TRISPHAT anion and in the solid state by X-ray diffraction.<sup>109, 111</sup> In a different manner, Le Lagadec et al. created planar chirality of the pincer moiety by using an unsymmetrical arene flanked by two OPR<sub>2</sub> donor sites.<sup>115</sup> Reaction of the resulting naphthoresorcinate-based pincer complex with the CpM'-cation afforded the corresponding half-sandwich pincer complex. This strategy allowed the synthesis of heterobimetallic complexes that incorporate the pairs Ru/Ni, Ru/Pd and Ru/Pt. The incorporation of Fe(II) and Cr was also possible, see Scheme 18.

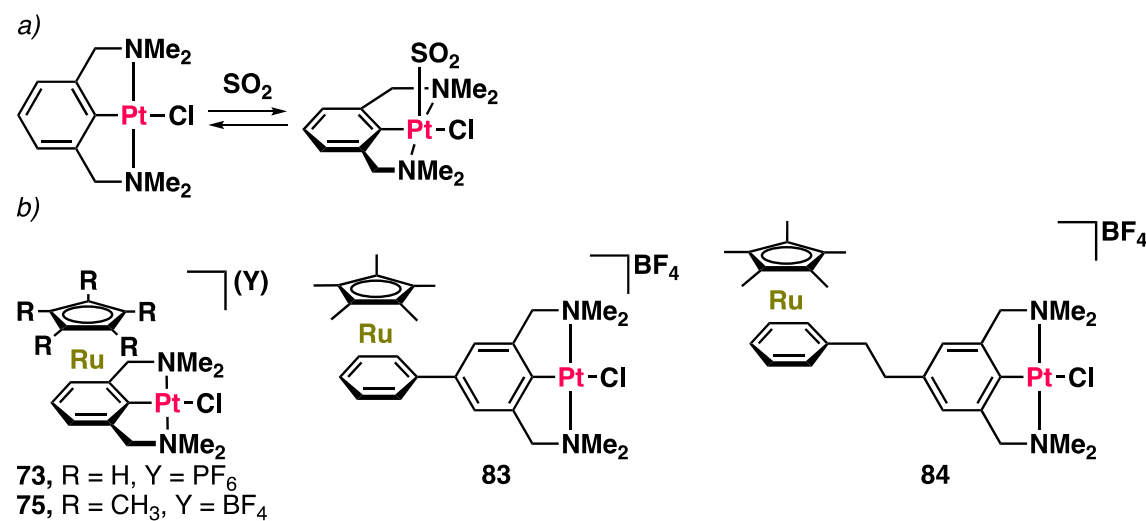
The extent of electronic communication in these heterobimetallic species in Scheme 19 could be established by computational chemistry, electrochemical measurements and by <sup>195</sup>Pt NMR. For the parent 4-substituted NCN-pincer platinum(II) chloride compounds extensive studies showed that the Pt-Cl grouping is a very strong EW grouping (comparable with NO<sub>2</sub>) whereas mesomerically it behaves as a very strong ER substituent; the overall effect (on 4-R, Hammett  $\sigma_H$ ) equals that of a NMe<sub>2</sub> group.<sup>116</sup> The result of a recent DFT calculation confirmed these conclusions.<sup>85</sup> Using these results and measuring the <sup>195</sup>Pt NMR shifts (under standard conditions) of **73** and **75** afforded the plot shown in Scheme 19. It revealed that coordination

of the Cp\*<sub>2</sub>Ru cation has a comparable effect as R = NO<sub>2</sub> but is a less strong arenophile than CpRu cation itself. However, both have EW effect comparable or even larger than that of a R = NO<sub>2</sub>, see the series of parent 4-substituted NCN-pincer-PtCl compounds in Scheme 19.<sup>86</sup>



**Scheme 19.** Extension of the  $\delta_{\text{Pt}} = f(\sigma_{\text{p}})$  linear relationship established for *para*-substituted NCN-Pt pincer complexes (solid black diamonds)<sup>117</sup> to  $\eta^6$ -modified complexes **73** and **75** (solid blue dots), figure adapted from ref 86.<sup>86</sup>

This conclusion was also supported by the tendency to bind the electrophiles I<sub>2</sub> and SO<sub>2</sub> in the series shown in Scheme 20. The parent NCN-pincer PtX compound is binding to both I<sub>2</sub> and SO<sub>2</sub> to provide NCNPtI( $\eta^1$ -I<sub>2</sub>) and NCNPtI( $\eta^1$ -SO<sub>2</sub>) complexes, respectively. This bonding involves coordination of the filled d<sub>z<sup>2</sup></sub> of Pt donating as an L-type ligand into the  $\sigma^*$  of either I<sub>2</sub> or SO<sub>2</sub>.<sup>114</sup>



**Scheme 20.** Reaction of SO<sub>2</sub> with; a) the parent NCN-pincer PtCl complex, and b) with one of the  $\eta^6$ ,  $\eta^1$ -NCN-pincer arene ruthenium-platinum complexes **73**, **75**, **83** or **84**.<sup>114</sup>

Calculations showed that  $\eta^1$ -coordination of  $\text{SO}_2$  to **73** is theoretically possible but leads to a 0.1 Å longer Pt–S bond and 21  $\text{kJ}\cdot\text{mol}^{-1}$  weaker binding energy for **73** than for **83**. An interpretation of this weakened platinum- $\text{SO}_2$  interaction was provided based on, 1) the electron-withdrawing effects of the  $\eta^6$ -coordinated ruthenium fragment (“through bond interaction”), and 2) the destabilizing charge–dipole interactions between the positive charge of the ruthenium center and the dipole moment of the  $\text{SO}_2$ -coordinated NCN-pincer platinum fragment (“through space interactions”).<sup>114</sup>

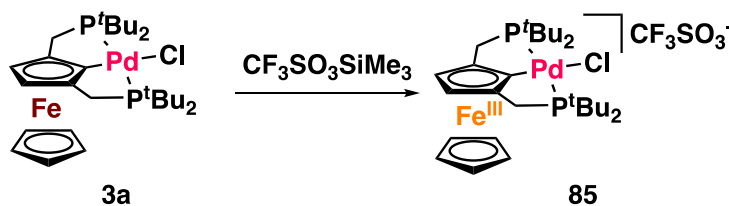
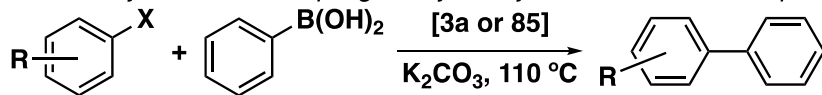
### 3. Catalysis

Heterobimetallic metallocene-based pincer complexes of type **A** have been used as catalyst in a range of different reactions (Scheme 21). Koridze and Sheloumov evaluated the catalytic activity of neutral and cationic palladium derivatives in the Suzuki-Miyaura cross-coupling using a triphasic organic/Aliquat 336/aqueous system.<sup>61</sup> Under these conditions the cationic complex performed better than the neutral species. This is probably due to a consequence of the modification of the electronic donor properties of the pincer ligand produced by the oxidized ferrocene fragment, which favored the reduction of Pd(II) to Pd(0), and thus the catalytic reaction may operate through a classical cycle of Pd(II)/Pd(0).

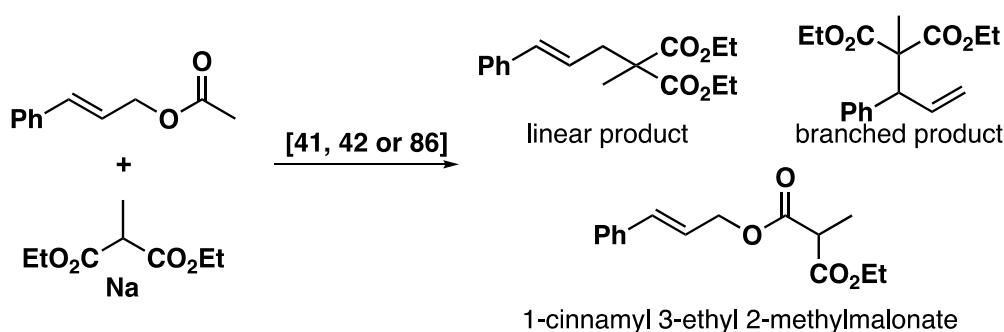
On the other hand, the catalytic activity of the ferrocenyl-based Pd(II)-pincer complexes of type **A'** (**41**, **42** and **86**) was tested in the allylic alkylation of (E)-3-phenyl-2-propenyl (cinnamyl) acetate with sodium diethyl 2-methylmalonate (Scheme 21).<sup>71</sup> This reaction affords three products: linear *trans*-(*E*) compound, the branched derivative and 1-cinnamyl-3-ethyl-2-methylmalonate. Both complexes **41** and **42** performed similarly yielding a 95 % conversion in 138 h. Complex **41** showed a slightly higher selectivity towards the formation of the linear product (molar ratio 84:5:11 vs 78:7:15 for **42**). However, ferrocenyl Schiff bases with a linear thioether moiety such as **86** showed higher catalytic activity.<sup>118</sup> The latter complex reached 90 % in 44 h, with a high selectivity (molar ratio linear/branched product 98.6:1.4).

Suzuki-Miyaura cross-coupling catalyzed by ferrocene-based Pd-pincer complexes<sup>61</sup>

View Article Online  
DOI: 10.1039/D1DT03870B



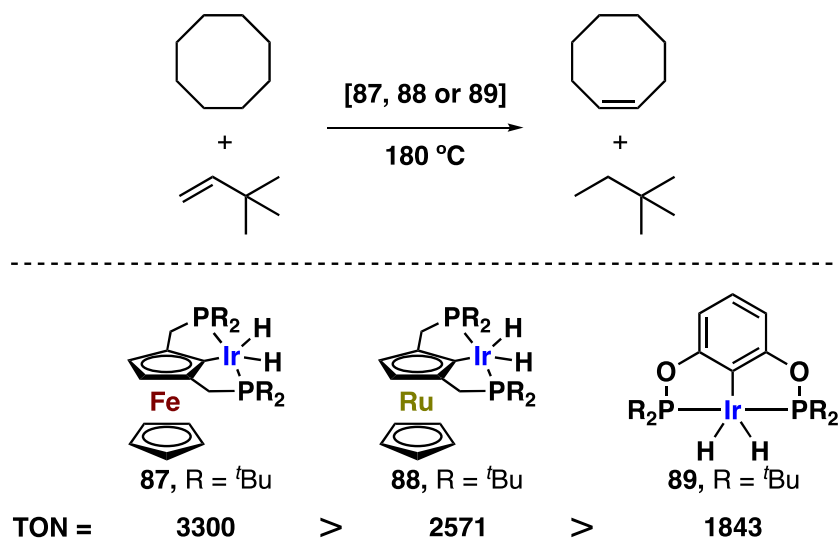
Allylic alkylation of cinnamyl acetate catalyzed by ferrocene-based Pd-pincer complexes<sup>71, 118</sup>



Complex	Linear/Branched/1-cinnamyl 3-ethyl 2-methylmalonate
86	98.6:1.4
41	84:5:11
42	78:7:15

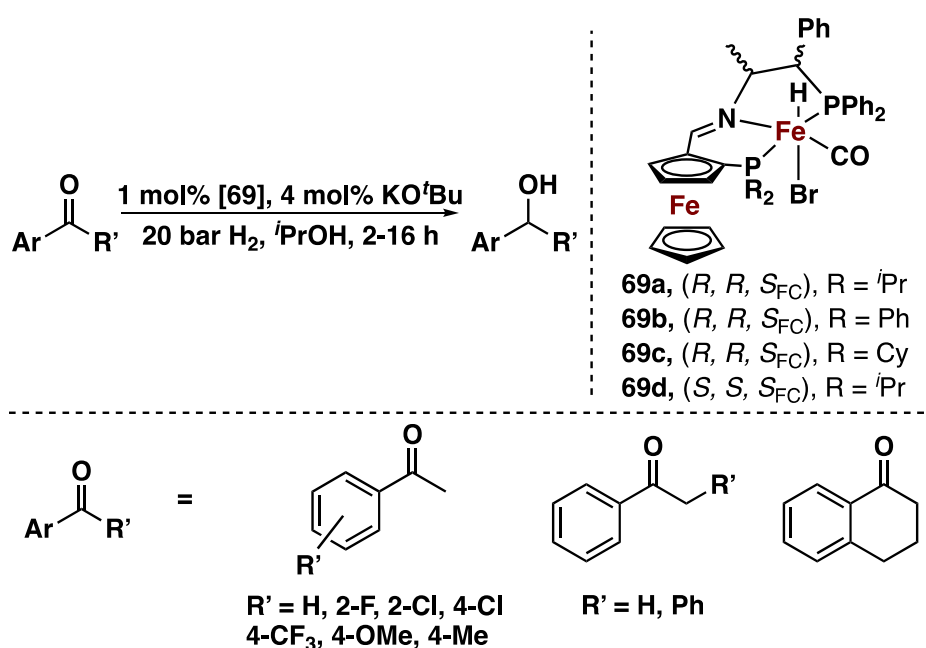
**Scheme 21.** Catalytic applications of ferrocene-based Pd-pincer complexes, see text.

Furthermore, the catalytic activity of the bimetallic dihydride complexes of type **A**, **87** and **88**, was evaluated in the transfer hydrogenation of *tert*-butylethylene with cyclooctane (Scheme 22).<sup>59</sup> The reaction was carried out at 180 °C for 8h. The ferrocene derivative showed a slightly better performance than the ruthenocene analogue, with TON's of 3300 vs 2571. Interestingly, these TONs values were higher than those values with the non-metallocene pincer-metal derivative. According to Koridze and co-workers, this better activity of the metallocene-pincer metal derivatives of type **A** is due to a combination of steric and electronic factors produced by the fixed and close M···M' arrangement achieved in type **A** bimetallics.<sup>59</sup>



**Scheme 22.** Comparison of the transfer hydrogenation reactions of tert-butylethylene with cyclooctane catalyzed by, respectively, the IrFe-, IrRu- bimetallic complexes with the activity of the mono Ir-based pincer complex.<sup>59</sup>

The catalytic activity of the, stereochemical pure, hydride compounds of type **C**, **69a-69d**, was evaluated in the asymmetric hydrogenation of ketones (Scheme 23).<sup>104</sup> The *S,S,S<sub>FC</sub>* diastereomer **69d** showed a 92% conversion but did not show any enantioselectivity. In contrast to this lack of stereoselectivity of **69d**, the *R,R,S<sub>FC</sub>* complexes, **69a** and **69c** displayed the best conversions and enantioselectivities, for example, using acetophenone and complex **69a** the conversion was 96% and 81% *ee*. Using acetophenone derivatives as substrate, complexes **69a** and **69c** performed excellently, but substrates bearing an electron-withdrawing group 4-R', such as -CF<sub>3</sub>, showed considerably decreased enantioselectivities.



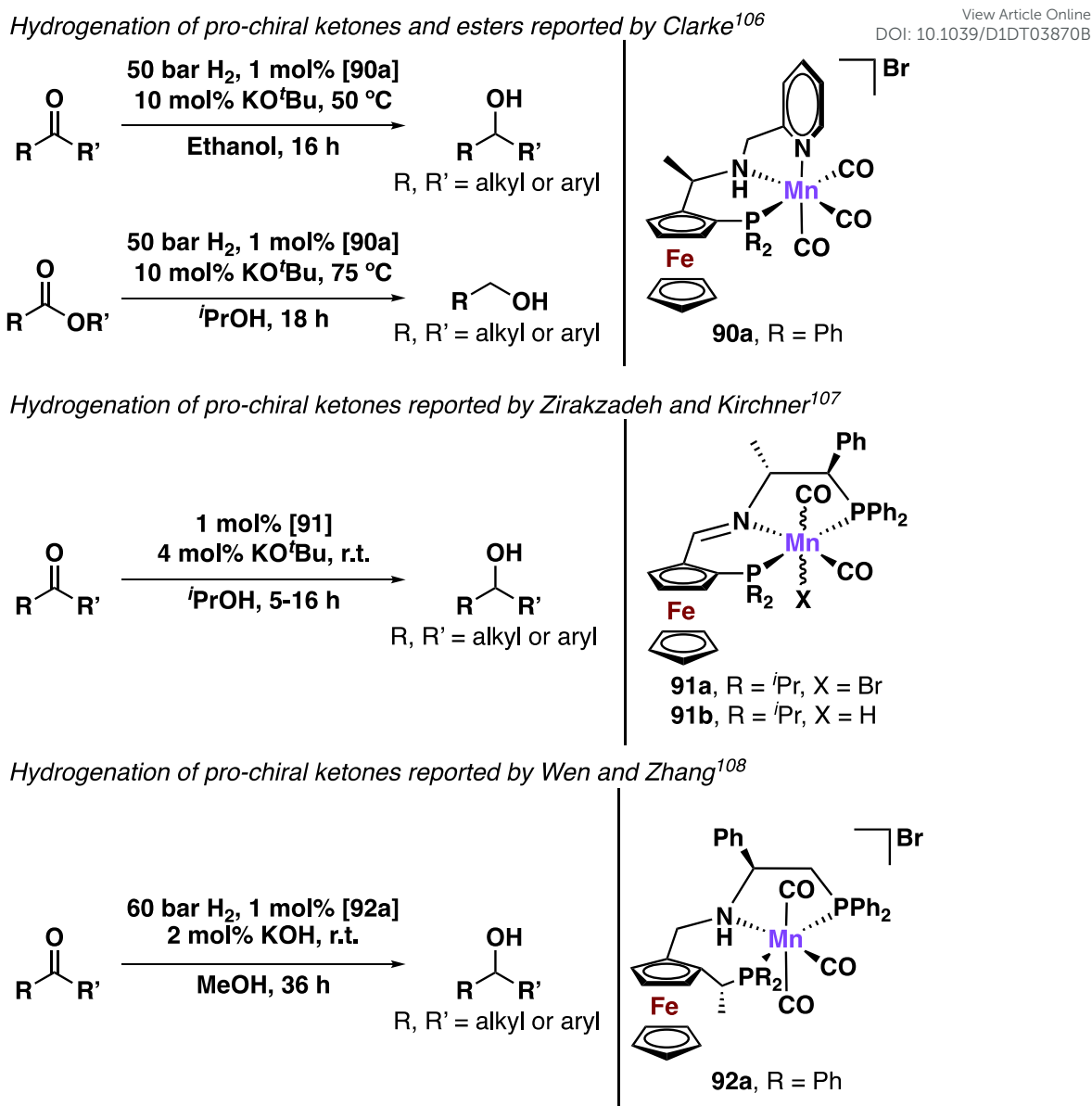
**Scheme 23.** Synthesis of secondary alcohols *via* hydrogenation of ketones.<sup>104</sup>



Recently, Mn pincer complexes have attracted much attention due to their remarkably high catalytic activity in hydrogenation/dehydrogenation processes. Recently, Clarke and co-workers described the catalytic activity of a bimetallic ferrocene-based Mn-PNN-pincer complex of type **C** (Scheme 24).<sup>106</sup> The complex showed an excellent catalytic activity in the hydrogenation of pro-chiral ketones, reaching 99 % yield, and *ee*'s between 61 and 97 %. The catalyst was also active in the hydrogenation of esters. In fact, the activity of such complex is comparable, and in some cases higher than that described for related catalysts.<sup>119, 120</sup> For example, the PNNNP-Mn pincer complex reported by Kempe and co-workers, reached a 82% yield for the hydrogenation of 2,2-dimethylpropiophenone in 24h using an hydrogen pressure of 20 bar and a temperature of 80 °C.<sup>120</sup> Whereas employing Clarke's conditions (Scheme 24) the yield was 99% in 16h.

In a similar approach, Zirakzadeh and Kirchner prepared a PNP Mn-pincer complex of type **C**, **91a**.<sup>107</sup> The reaction of this complex with [NaBH<sub>4</sub>] affords a mixture of isomer hydride species, **91b**, due to the exchange reaction of one bromine by a hydride ligand. Complex **91a** was tested in the asymmetric transfer hydrogenation and asymmetric hydrogenation reactions of acetophenone (Scheme 24). As the authors observed that the reactions produced the same conversions and *ee*'s both in the absence and in the presence of dihydrogen it was concluded that *iso*-propanol is the true *hydrogen donor* in this process. The screening of different substrates afforded conversions and *ee*'s up to 96 % and 86 %, respectively. Preliminary DFT calculations, indicated that the actual active species is the hydride specie **91b**. The latter intermediate which is generated under the applied reaction conditions proceeds through an outer-sphere mechanistic pathway.

In 2020, Wen and Zhang reported a series of Mn PNP-pincer complexes of type **C** and evaluated their catalytic activity in the hydrogenation of acetophenone with dihydrogen in methanol (Scheme 24).<sup>108</sup> The most active catalyst reached a TON and *ee* up to 2000 and 99 %. According to DFT calculations, the flexibility of the 5-membered ring in type **C** complexes is responsible for the observed high enantiomeric induction.



**Scheme 24.** Hydrogenation reactions catalyzed by metallocene-based Mn-pincer complexes.

#### 4. Conclusions

Four likely paths to merge a metallocene and a pincer-metal building block, see **A**, **A'**, **B** and **C**, in **Scheme 1**, were explored to provide an answer to the question raised in the title of our perspective. For each of these approaches representative examples from the literature, regarding their synthesis, characterization, and reactivity, specifically as (pre)catalytic material in organic synthesis, were displayed and discussed.

Incorporation of different (organometallic) functionalities, either complementary or orthogonally, in one molecule can be of interest, for example, as it allows the development of materials in which these functionalities function as construction sites (e.g. the synthesis of MOF's), of catalysts in which each of the sites catalyze different, orthogonal, conversions or provide to the overall molecular assembly distinct stereochemical properties.

The closest possible *integration* of the metallocene and (*cyclopentadienyl*)pincer-metal motifs is present in mergers **A** and to a lesser extent also in **A'**. Whereas in **A** the two pincer arms, flanking the  $C^{Cp}-M$  bond, are directly fixed in 2- and 5-positions, it is in **A'**, having a  $CH_2DCH_2CH_2D'$  in the 2-position that installs, instead of a *trans*- $D,C^{Cp},D'$ , present in **A**, a *cis*- $C^{Cp},D,D'$  pincer motif. An obvious consequence of the *cis*- $C^{Cp},D,D'$  arrangement is that in **A'** the *cis*-pincer ligand arrangement can easily switch back and forth between terdentate *cis*- $C^{Cp},D,D'$  coordination and a bidentate  $C^{Cp},D$ -binding, with a *dangling*  $D'$ -donor site. A common, unique, aspect of **A** and **A'** is the “fixed” arrangement of the (metallocene)- $M$  and (pincer)- $M'$  metal sites. This is reflected by the *electronic communication/Coulombic effects* observed in the  $M \cdots M'$  manifold which can be manipulated by changing the oxidation state of  $M$ , *i.e.*, oxidation of  $M$  enhances the electron withdrawing effect on  $M'$  thereby affecting the reactivity of  $M'$ , *e.g.* when involved as catalyst, see Scheme 21. Finally note that both  $M$  and  $M'$  interact electronically with the  $C^{Cp}$ -anion that eventually promotes electronic communication, *vide infra*.

Merger **B** can be considered as an (*aryl*)pincer- $M'$  motif carrying a metallocene- $M$  motif as a *para*-substituent. The  $M \cdots M'$  electronic communication will be through mesomeric and inductive effects exerted by the metallocene substituent involving the aryl's  $\sigma$ - and  $\pi$ -system, cf. Scheme 19, *vide infra*. Notably, this means that in **B** similar as in **A** and **A'** a direct through bond electronic  $M \cdots M'$  communication is possible but that  $M$  and  $M'$  are too far separated for through space interaction. Whereas the metallocene motif in **B** can be seen as a substituent to the arylpincer motif, in **C** the metallocene is just involved in the connecting chain between  $D$  and  $D'$  of a terdentate, neutral  $D, D', D''$ -pincer motif. In practice, the chelate  $D, D'$ -bidentate bonding to  $M'$  is stronger than the tridentate  $D, D', D''$  bonding, *i.e.*, like observed for **A'** the  $D''$ -donor site acts generally as a dangling ligand, see Scheme 15.

Furthermore, metallocene-pincer metal sandwich compounds can be easily synthesized by reacting arenophiles, such as  $[CpM]^+$  and  $[Cp^*M]^+$ , with an aryl-pincer metal complex. When the aryl-pincer metal complex has a non-symmetrical backbone, this approach provides a suitable and accessible strategy to create diastereomeric pincer-metal sandwich compounds, providing an excellent opportunity for the development of new, stereoselective catalytic systems. Finally, the  $\eta^6$ -binding of the arenophile to the pincer backbone may allow the modification of the electronic properties of the pincer ligand, due to its electron-withdrawing character.

## 5. Outlook

One of the interesting and exciting aspects of the merger of metallocene- and pincer-metal motifs are its *stereochemical consequences*, *i.e.*, as both motifs are *platforms*, that have *planar chirality*, their merger generally creates a mixture of stereoisomeric, bimetallic species. As in a number of cases it has already been shown that enantio- and diastereo-isomerically pure bimetallic species are formed and isolated, their application in stereoselective catalysis is obvious, see Scheme 24. A switch from *metallocene to half sandwich* complexes brings about another type of merger between (aryl)pincer  $M'$  and an arenophile  $[CpM]^+$  *via* a  $\eta^6$ -type of

bonding, see Scheme 17 and 18. The resulting bimetallic, monocationic complexes of type A can be obtained with high diastereo-selectivity and enantiopurity by using the chiral TRISPHAT anion, see Scheme 18. This very versatile approach, in view of the tremendous diversity of non-symmetrical pincer-metal complexes described up to date, provides a facile access to diastereomeric metallocene-pincer metal sandwich compounds.

In the designs reported above the second cyclopentadienyl ring was solely either a Cp or Cp\* grouping. However, this ring could also be used, after proper substitution, in *material synthesis*, for example, for anchoring the bimetallic species to an electrode or nanosized species like dendrimers, or to an electrode surface. Recently, the latter application has been reported.<sup>121</sup> Moreover, as also the pincer metal system is prone to become involved in non-covalent interactions, by introduction of a suitable functional group at the second Cp-ring, the formation of polymeric and other functional materials could be envisaged.

### Acknowledgment

H.V. thanks CONACYT (CVU: 410706) and Generalitat de Catalunya (Beatriu de Pinós H<sub>2</sub>O<sub>2</sub> MSCA-Cofund 2019-BP-0080). D.M.-M. thanks the generous financial support of PAPIIT-DGAPA-UNAM (PAPIIT IN210520), CONACYT A1-S-33933 and FORDECYT-PRONACES FON.INST 22/2020 (FOINS 307152).

### References

1. A. D. McNaught and A. Wilkinson, eds., *IUPAC. Compendium of Chemical Terminology*, Blackwell Scientific Publications, Oxford, 2019.
2. T. J. Kealy and P. L. Pauson, *Nature*, 1951, **168**, 1039-1040.
3. S. A. Miller, J. A. Tebboth and J. F. Tremaine, *J. Chem. Soc.*, 1952, **1952**, 632-635.
4. G. Wilkinson, M. Rosenblum, M. C. Whiting and R. B. Woodward, *J. Am. Chem. Soc.*, 1952, **74**, 2125-2126.
5. E. O. Fischer and W. Pfab, *Z. Naturforsch. B*, 1952, **7**, 377-379.
6. R. Sun, L. Wang, H. Yu, Z.-u. Abdin, Y. Chen, J. Huang and R. Tong, *Organometallics*, 2014, **33**, 4560-4573.
7. A. Togni and R. Halterman, *Metallocenes: Synthesis Reactivity Applications*, Wiley-VCH, 1998.
8. S. S. Braga and A. M. S. Silva, *Organometallics*, 2013, **32**, 5626-5639.
9. X. Liu, Y. Jin, T. Liu, S. Yang, M. Zhou, W. Wang and H. Yu, *ACS Biomater. Sci. Eng.*, 2020, **6**, 4834-4845.
10. P. F. Salas, C. Herrmann and C. Orvig, *Chem. Rev.*, 2013, **113**, 3450-3492.
11. R. Wang, H. Chen, W. Yan, M. Zheng, T. Zhang and Y. Zhang, *Eur. J. Med. Chem.*, 2020, **190**, 112109.
12. L. Fabbrizzi, *ChemTexts*, 2020, **6**, 22.
13. D. Astruc, *Eur. J. Inorg. Chem.*, 2017, **2017**, 6-29.
14. M. G. Walawalkar, P. Pandey and R. Murugavel, *Angew. Chem. Int. Ed.*, 2021, **60**, 12632-12635.
15. F. Dumur, *Eur. Polym. J.*, 2021, **147**, 110328.
16. M. L. Pegis, C. F. Wise, D. J. Martin and J. M. Mayer, *Chem. Rev.*, 2018, **118**, 2340-2391.
17. P. Neumann, H. Dib, A. M. Caminade and E. Hey-Hawkins, *Angew. Chem. Int. Ed.*, 2015, **54**, 311-314.

18. R. Gomez Arrayas, J. Adrio and J. C. Carretero, *Angew. Chem. Int. Ed.*, 2006, **45**, 7674-7715. View Article Online  
DOI: 10.1039/B5DT03870B
19. R. Peters, D. F. Fischer and S. Jautze, *Top. Organomet. Chem.*, 2011, **33**, 139-175.
20. L. Cunningham, A. Benson and P. J. Guiry, *Org. Biomol. Chem*, 2020, **18**, 9329-9370.
21. A. Togni, C. Breutel, A. Schnyder, F. Spindler, H. Landert and A. Tijani, *J. Am. Chem. Soc.*, 1994, **116**, 4062-4066.
22. O. B. Sutcliffe and M. R. Bryce, *Tetrahedron: Asymmetry*, 2003, **14**, 2297-2325.
23. J.-C. Zhu, D.-X. Cui, Y.-D. Li, R. Jiang, W.-P. Chen and P.-A. Wang, *ChemCatChem*, 2018, **10**, 907-919.
24. U. Rosenthal, *Organometallics*, 2020, **39**, 4403-4414.
25. A. E. Hamielec and J. B. P. Soares, in *Polypropylene*, ed. K.-K. J., Springer, Dordrecht, 1999, vol. 2, pp. 446-453.
26. W. Kaminsky, *J. Polym. Sci., Part A: Polym. Chem.*, 2004, **42**, 3911-3921.
27. S. Kumar, B. Z. Dholakiya and R. Jangir, *J. Organomet. Chem.*, 2021, **953**, 122066.
28. W. Kaminsky, A. Funck and H. Hahnsen, *Dalton Trans.*, 2009, **2009**, 8803-8810.
29. J. Pinkas and M. Lamač, *Coord. Chem. Rev.*, 2015, **296**, 45-90.
30. I. E. Nifant'ev, P. V. Ivchenko and A. A. Vinogradov, *Coord. Chem. Rev.*, 2021, **426**, 213515.
31. C. J. Moulton and B. L. Shaw, *J. Chem. Soc., Dalton Trans.*, 1976, **1976**, 1020-1024.
32. J. Nevarez, A. Turmo, J. Hu and R. P. Hausinger, *ChemCatChem*, 2020, **12**, 4242-4254.
33. H. Valdés, J. M. Germán-Acacio and D. Morales-Morales, in *Organic Materials as Smart Nanocarriers for Drug Delivery*, ed. A. M. Grumezescu, Elsevier - William Andrew, 2018, DOI: 10.1016/B978-0-12-813663-8.00007-5, pp. 245-291.
34. M. A. W. Lawrence, K.-A. Green, P. N. Nelson and S. C. Lorraine, *Polyhedron*, 2018, **143**, 11-27.
35. H. Valdés, M. A. García-Eleno, D. Canseco-Gonzalez and D. Morales-Morales, *ChemCatChem*, 2018, **10**, 3136-3172.
36. D. Morales-Morales, *Rev. Soc. Quim. Mex.*, 2004, **48**, 338-346.
37. K. J. Szabó and O. F. Wendt, *Pincer and Pincer-Type Complexes: Applications in Organic Synthesis and Catalysis*, 2014.
38. D. Morales-Morales, *Pincer Compounds Chemistry and Applications*, Elsevier, First edn., 2018.
39. H. Valdés, E. Rufino-Felipe, G. van Koten and D. Morales-Morales, *Eur. J. Inorg. Chem.*, 2020, **2020**, 4418-4424.
40. H. Valdés, E. Rufino-Felipe and D. Morales-Morales, *J. Organomet. Chem.*, 2019, **898**, 120864.
41. G. Bauer and X. Hu, *Inorg. Chem. Front.*, 2016, **3**, 741-765.
42. N. Selander and K. J. Szabó, *Chem. Rev.*, 2011, **111**, 2048-2076.
43. K. J. Szabó, *Top. Organomet. Chem.*, 2013, **40**, 203-242.
44. D. M. Roddick, *Top. Organomet. Chem.*, 2013, **40**, 49-88.
45. C. Gunanathan and D. Milstein, *Chem. Rev.*, 2014, **114**, 12024-12087.
46. J. Choi, A. H. R. MacArthur, M. Brookhart and A. S. Goldman, *Chem. Rev.*, 2011, **111**, 1761-1779.
47. H. Li, B. Zheng and K. W. Huang, *Coord. Chem. Rev.*, 2015, **293-294**, 116-138.
48. H. A. Younus, N. Ahmad, W. Su and F. Verpoort, *Coord. Chem. Rev.*, 2014, **276**, 112-152.
49. I. E. Nifant'ev and P. V. Ivchenko, *Adv. Synth. Catal.*, 2020, **362**, 3727-3767.
50. A. A. Koridze, A. M. Sheloumov, S. A. Kuklin, V. Y. Lagunova, I. I. Petukhova, F. M. Dolgushin, M. G. Ezernitskaya, P. V. Petrovskii, A. A. Macharashvili and R. V. Chedia, *Russ. Chem. Bull.*, 2002, **51**, 1077-1078.

51. E. J. Farrington, E. Martinez Viviente, B. S. Williams, G. van Koten and J. M. Brown, *Chem. Commun.*, 2002, **2002**, 308-309. View Article Online  
DOI: 10.1039/01b003870b
52. A. A. Koridze, S. A. Kuklin, A. M. Sheloumov, M. V. Kondrashov, F. M. Dolgushin, A. S. Peregudov and P. V. Petrovskii, *Russ. Chem. Bull.*, 2003, **52**, 2754-2756.
53. B. Vabre, M. L. Lambert, A. Petit, D. H. Ess and D. Zargarian, *Organometallics*, 2012, **31**, 6041-6053.
54. A. M. Sheloumov, F. M. Dolgushin, M. V. Kondrashov, P. V. Petrovskii, K. A. Barbakadze, O. I. Lekashvili and A. A. Koridze, *Russ. Chem. Bull.*, 2007, **56**, 1757-1764.
55. S. V. Safronov, A. M. Sheloumov, A. Z. Kreindlin, A. A. Kamyshova, F. M. Dolgushin, A. F. Smolyakov, P. V. Petrovskii, M. G. Ezernitskaya and A. A. Koridze, *Russ. Chem. Bull.*, 2010, **59**, 1740-1744.
56. S. V. Safronov and A. A. Koridze, *Russ. Chem. Bull.*, 2018, **67**, 1247-1250.
57. A. A. Koridze, S. A. Kuklin, A. M. Sheloumov, F. M. Dolgushin, V. Y. Lagunova, I. I. Petukhova, M. G. Ezernitskaya, A. S. Peregudov, P. V. Petrovskii, E. V. Vorontsov, M. Baya and R. Poli, *Organometallics*, 2004, **23**, 4585-4593.
58. S. Pérez, C. López, A. Caubet, X. Solans and M. Font-Bardía, *Eur. J. Inorg. Chem.*, 2008, **2008**, 1599-1612.
59. S. A. Kuklin, A. M. Sheloumov, F. M. Dolgushin, M. G. Ezernitskaya, A. S. Peregudov, P. V. Petrovskii and A. A. Koridze, *Organometallics*, 2006, **25**, 5466-5476.
60. A. V. Polukeev, S. A. Kuklin, P. V. Petrovskii, S. M. Peregudova, A. F. Smol'yakov, F. M. Dolgushin and A. A. Koridze, *Dalton Trans.*, 2011, **40**, 7201-7209.
61. A. M. Sheloumov, P. Tundo, F. M. Dolgushin and A. A. Koridze, *Eur. J. Inorg. Chem.*, 2008, **2008**, 572-576.
62. A. A. Koridze, *Russ. Chem. Bull.*, 2003, **52**, 516-517.
63. A. V. Polezhaev, M. G. Ezernitskaya and A. A. Koridze, *Inorg. Chim. Acta*, 2019, **496**, 118844.
64. A. A. Koridze, S. A. Kuklin, A. M. Sheloumov, M. V. Kondrashov, F. M. Dolgushin, M. G. Ezernitskaya, P. V. Petrovskii and E. V. Vorontsov, *Russ. Chem. Bull.*, 2003, **52**, 2757-2759.
65. S. V. Safronov, E. S. Osipova, Y. V. Nelyubina, O. A. Filippov, I. G. Barakovskaya, N. V. Belkova and E. S. Shubina, *Molecules*, 2020, **25**, 2236.
66. S. V. Safronov, E. I. Gutsul, I. E. Golub, F. M. Dolgushin, Y. V. Nelubina, O. A. Filippov, L. M. Epstein, A. S. Peregudov, N. V. Belkova and E. S. Shubina, *Dalton Trans.*, 2019, **48**, 12720-12729.
67. M. Gawron, B. Nayyar, C. Krabbe, M. Lutter and K. Jurkschat, *Eur. J. Inorg. Chem.*, 2019, **2019**, 1799-1809.
68. B. Nayyar, S. Koop, M. Lutter and K. Jurkschat, *Eur. J. Inorg. Chem.*, 2017, **2017**, 3233-3238.
69. A. Avila-Sorroza, F. Estudiante-Negrete, S. Hernández-Ortega, R. A. Toscano and D. Morales-Morales, *Inorg. Chim. Acta*, 2010, **363**, 1262-1268.
70. C. López, R. Bosque, S. Pérez, A. Roig, E. Molins, X. Solans and M. Font-Bardía, *J. Organomet. Chem.*, 2006, **691**, 475-484.
71. D. Pou, C. López, S. Pérez, X. Solans, M. Font-Bardía, P. W. N. M. van Leeuwen and G. P. F. van Strijdonck, *Eur. J. Inorg. Chem.*, 2010, **2010**, 1642-1648.
72. C. López, M. Salmi, A. Mas, P. Piotrowski, M. Font Bardía and T. Calvet, *Eur. J. Inorg. Chem.*, 2012, **2012**, 1702-1709.
73. A. Bahsoun, J. Dehand, M. Pfeffer, M. Zinsius, S.-E. Bouaoud and G. Le Borgne, *J. Chem. Soc., Dalton Trans.*, 1979, **1979**, 547-556.
74. F. Maassarani, M. Pfeffer and G. Le Borgne, *Organometallics*, 1987, **6**, 2029-2043.

75. M. Pfeffer and M. A. Rotteveel, *Recl. Trav. Chim. Pays-Bas*, 1989, **108**, 317-318. View Article Online  
DOI: 10.1039/D1DT03870B
76. M. Pfeffer, M. A. Rotteveel, J.-P. Sutter, A. De Cian and J. Fischer, *J. Organomet. Chem.*, 1989, **371**, C21-C25.
77. M. T. Pereira, M. Pfeffer and M. A. Rotteveel, *J. Organomet. Chem.*, 1989, **375**, 139-145.
78. M. Pfeffer, *Recl. Trav. Chim. Pays-Bas*, 1990, **109**, 567-576.
79. M. Pfeffer, M. A. Rotteveel, A. de Cian, J. Fisher and G. le Borgne, *J. Organomet. Chem.*, 1991, **413**, C15-C19.
80. M. Pfeffer, J.-P. Sutter, M. A. Rotteveel, A. D. Cian and J. Fischer, *Tetrahedron*, 1992, **48**, 2427-2440.
81. F. Maassarani, M. Pfeffer, J. Spencer and E. Wehman, *J. Organomet. Chem.*, 1994, **466**, 265-271.
82. J. Spencer and M. Pfeffer, *Adv. Metal-Org. Chem.*, 1998, **6**, 103-144.
83. J. Chengebroyen, M. Linke, M. Robitzer, C. Sirlin and M. Pfeffer, *J. Organomet. Chem.*, 2003, **687**, 313-321.
84. S. Köcher, G. P. M. van Klink, G. van Koten and H. Lang, *J. Organomet. Chem.*, 2003, **684**, 230-234.
85. A. J. Canty, A. Ariafard and G. van Koten, *Chem. Eur. J.*, 2020, **26**, 15629-15635.
86. S. Bonnet, M. Lutz, A. L. Spek, G. v. Koten and R. J. M. Klein Gebbink, *Organometallics*, 2008, **27**, 159-162.
87. S. Köcher, M. Lutz, A. L. Spek, R. Prasad, G. P. M. van Klink, G. van Koten and H. Lang, *Inorg. Chim. Acta*, 2006, **359**, 4454-4462.
88. H. Lang, R. Packheiser and B. Walfort, *Organometallics*, 2006, **25**, 1836-1850.
89. A. J. Canty and A. Ariafard, *Organometallics*, 2021, **40**, 1262-1269.
90. W. G. Whitehurst and M. J. Gaunt, *J. Am. Chem. Soc.*, 2020, **142**, 14169-14177.
91. S. Köcher, G. P. M. van Klink, G. van Koten and H. Lang, *J. Organomet. Chem.*, 2006, **691**, 3319-3324.
92. S. Köcher, B. Walfort, G. P. M. van Klink, G. van Koten and H. Lang, *J. Organomet. Chem.*, 2006, **691**, 3955-3961.
93. M. Albrecht, M. Lutz, A. L. Spek and G. van Koten, *Nature*, 2000, **406**, 970-974.
94. M. Albrecht, M. Schlupp, J. Bargon and G. van Koten, *Chem. Commun.*, 2001, **2001**, 1874-1875.
95. M. Albrecht, R. A. Gossage, U. Frey, A. W. Ehlers, E. J. Baerends, A. E. Merbach and G. van Koten, *Inorg. Chem.*, 2001, **40**, 850-855.
96. M. Albrecht, G. Rodriguez, J. Schoenmaker and G. van Koten, *Org. Lett.*, 2000, **2**, 3461-3464.
97. M. Albrecht and G. van Koten, *Adv. Mater.*, 1999, **11**, 171-174.
98. S. Kuriyama, K. Arashiba, K. Nakajima, H. Tanaka, K. Yoshizawa and Y. Nishibayashi, *Chem. Sci.*, 2015, **6**, 3940-3951.
99. T. Itabashi, K. Arashiba, H. Tanaka, A. Konomi, A. Eizawa, K. Nakajima, K. Yoshizawa and Y. Nishibayashi, *Organometallics*, 2019, **38**, 2863-2872.
100. T. Itabashi, I. Mori, K. Arashiba, A. Eizawa, K. Nakajima and Y. Nishibayashi, *Dalton Trans.*, 2019, **48**, 3182-3186.
101. K. Arashiba, Y. Miyake and Y. Nishibayashi, *Nat. Chem.*, 2011, **3**, 120-125.
102. E. Kinoshita, K. Arashiba, S. Kuriyama, Y. Miyake, R. Shimazaki, H. Nakanishi and Y. Nishibayashi, *Organometallics*, 2012, **31**, 8437-8443.
103. S. Kuriyama, K. Arashiba, K. Nakajima, H. Tanaka, N. Kamaru, K. Yoshizawa and Y. Nishibayashi, *J. Am. Chem. Soc.*, 2014, **136**, 9719-9731.
104. A. Zirakzadeh, K. Kirchner, A. Roller, B. Stöger, M. Widhalm and R. H. Morris, *Organometallics*, 2016, **35**, 3781-3787.

105. A. Zirakzadeh, K. Kirchner, A. Roller, B. Stöger, M. D. Carvalho and L. P. Ferreira, *RSC Adv.*, 2016, **6**, 11840-11847. View Article Online  
DOI: 10.1039/D1TB03870B
106. M. B. Widegren, G. J. Harkness, A. M. Z. Slawin, D. B. Cordes and M. L. Clarke, *Angew. Chem. Int. Ed.*, 2017, **56**, 5825-5828.
107. A. Zirakzadeh, S. R. M. M. de Aguiar, B. Stöger, M. Widhalm and K. Kirchner, *ChemCatChem*, 2017, **9**, 1744-1748.
108. L. Zeng, H. Yang, M. Zhao, J. Wen, J. H. R. Tucker and X. Zhang, *ACS Catalysis*, 2020, **10**, 13794-13799.
109. S. Bonnet, J. Li, M. A. Siegler, L. S. von Chrzanowski, A. L. Spek, G. van Koten and R. J. Klein Gebbink, *Chem. Eur. J.*, 2009, **15**, 3340-3343.
110. S. Bonnet, J. H. van Lenthe, M. A. Siegler, A. L. Spek, G. van Koten and R. J. M. K. Gebbink, *Organometallics*, 2009, **28**, 2325-2333.
111. S. Bonnet, M. Lutz, A. L. Spek, G. van Koten and R. J. M. Klein Gebbink, *Organometallics*, 2010, **29**, 1157-1167.
112. S. Bonnet, M. A. Siegler, J. H. van Lenthe, M. Lutz, A. L. Spek, G. van Koten and R. J. M. Klein Gebbink, *Eur. J. Inorg. Chem.*, 2010, **2010**, 4667-4677.
113. M. A. Siegler, S. Bonnet, A. M. M. Schreurs, R. J. M. Klein Gebbink, G. van Koten and A. L. Spek, *J. Chem. Crystallogr.*, 2010, **40**, 753-760.
114. S. Bonnet, J. H. van Lenthe, H. J. van Dam, G. van Koten and R. J. Klein Gebbink, *Dalton Trans.*, 2011, **40**, 2542-2548.
115. N. Á. Espinosa-Jalapa, S. Hernández-Ortega, X.-F. Le Goff, D. Morales-Morales, J.-P. Djukic and R. Le Lagadec, *Organometallics*, 2013, **32**, 2661-2673.
116. G. D. Batema, M. Lutz, A. L. Spek, C. A. van Walree, G. P. van Klink and G. van Koten, *Dalton Trans.*, 2014, **43**, 12200-12209.
117. M. Q. Slagt, G. Rodriguez, M. M. Grutters, R. J. Klein Gebbink, W. Klopper, L. W. Jenneskens, M. Lutz, A. L. Spek and G. van Koten, *Chem. Eur. J.*, 2004, **10**, 1331-1344.
118. C. López, S. Pérez, X. Solans, M. Font-Bardía, A. Roig, E. Molins, L. van and S. van, *Organometallics*, 2007, **26**, 571-576.
119. S. Elangovan, C. Topf, S. Fischer, H. Jiao, A. Spannenberg, W. Baumann, R. Ludwig, K. Junge and M. Beller, *J. Am. Chem. Soc.*, 2016, **138**, 8809-8814.
120. F. Kallmeier, T. Irrgang, T. Dietel and R. Kempe, *Angew. Chem. Int. Ed.*, 2016, **55**, 11806-11809.
121. K. Barman, X. Wang, R. Jia, G. Askarova, G. Hu and M. V. Mirkin, *J. Am. Chem. Soc.*, 2021, **143**, 17344-17347.